



The Effect of Deposited Particulate Matter on the Mobility of Contaminants in the Surficial Soils of Flin Flon, Manitoba, Canada

Michael Schindler · Max Schreckenbach · Tessa Warkentine ·
Sisara Samaradiwakara · Xinyang Li

Received: 12 April 2024 / Accepted: 3 June 2024 / Published online: 14 June 2024
© The Author(s), under exclusive licence to Springer Nature Switzerland AG 2024

Abstract The mobility of metals in surficial soils is among many factors controlled by the solubility of particulate matter (PM) deposited on their surface. This paper shows that the deposition of smaller, more soluble, Cu-, Zn- and Pb-bearing PM likely led to a higher mobility of these elements in finer textured soils with higher pH than in more acidic coarser textured soils with higher proportions of organic matter and gravel. This paradox (and novelty) is unraveled in the smelter-impacted soils of Flin Flon, Manitoba, Canada where the wet and dry deposition of particulates emitted by the smelter led to a smelter-shadow effect in close proximity to the smelter. Two pedons, one within and one outside of the smelter shadow are sampled parallel to the prevailing NW-SE wind direction. Leaching experiments and chemical, mineralogical, and textural analyses of these soils indicate a higher mobility of Cu, Pb and Zn in a limed soil within the smelter shadow and a higher mobility of As in an acidic soil immediately outside of the smelter shadow. The former observation is likely a result of the enhanced wet deposition of smaller more soluble Cu-, Pb- and Zn-sulfate and arsenate particles

closer to the smelter. The latter observation is explained with the depletion of Fe-(hydr)oxides in the surficial soils under acidic pH conditions. The leaching experiments also show that the proportions of As, Cu, Pb and Zn in colloidal fractions increase in the sequence of $Zn \leq As < Cu < Pb$, reflecting the affinity of these metals towards mineral and organic matter surfaces.

Keywords Metal mobility · Smelter · Contaminated soils · Colloids · Leaching · Shadow effect

1 Introduction

Soils are vital components of our lives, and with an increasing global population and the consequent demands placed on arable land, a reduction in the abundance of healthy and productive soils is fast becoming a reality. Acidification of soils (i.e., $pH < 5.5$) and the emission of metal-bearing particulate matter (PM) from industrial processes are detrimental to crop production and lead to increased soil degradation (Freedman & Hutchinson, 2011; Ritchie, 1994; Samac & Tesfaye, 2003). In particular, emissions of sulfuric acid, sulfur dioxide, and PM have created technogenic landscapes on a worldwide scale (Koptsik, 2014), notable examples of which include areas in southern Italy (Terzano et al., 2007); southwestern Spain (Chopin & Alloway, 2007); the Kola Peninsula, Russia (Gregurek et al., 1998); Zlatna, Romania (Williamson et al., 2012); the United States of America (e.g. Colorado and Montana (Burt

Supplementary Information The online version contains supplementary material available at <https://doi.org/10.1007/s11270-024-07248-5>.

M. Schindler (✉) · M. Schreckenbach · T. Warkentine ·
S. Samaradiwakara · X. Li
Department of Earth Sciences, University of Manitoba,
Winnipeg, Manitoba R3T2N2, Canada
e-mail: Michael.schindler@umanitoba.ca

et al., 2011; Burt et al., 2003); and Canada (Sudbury, Ontario (Meadows & Watmough, 2012) and Flin Flon, Manitoba (Zoltai, 1988)).

Many of the technogenic landscapes are products of smelter activities. Smelters are considered point sources of metal(loid) pollution where the concentration of emitted elements commonly decreases in surficial environments with distance from the source and with depth in the soil (Briffa et al., 2020). Although the smelter emissions disperse in all directions, zones of high metal contamination are often elliptical and elongated in the prevailing wind direction (McMartin et al., 1999; Zoltai, 1988). In some

cases, the height of the smelter stack combined with moderate-strong winds give rise to a shadow effect (Caplette et al., 2015; de Caritat et al., 1997), which results in a lower degree of contamination near the smelter stack (Fig. 1a). This contamination shadow is followed by a sharp increase at a fairly small distance from the stack, usually 100s of m to a few km, after which there is a gradual decrease of the metal(loid)s in the geological medium (soils, lakes, rock coatings) with distance to the smelter (de Caritat et al., 1997).

After deposition, the metal(loid)-bearing PM mixes with soil constituents such as leaves, plant litter and mineral grains (Jadoon & Schindler, 2022;

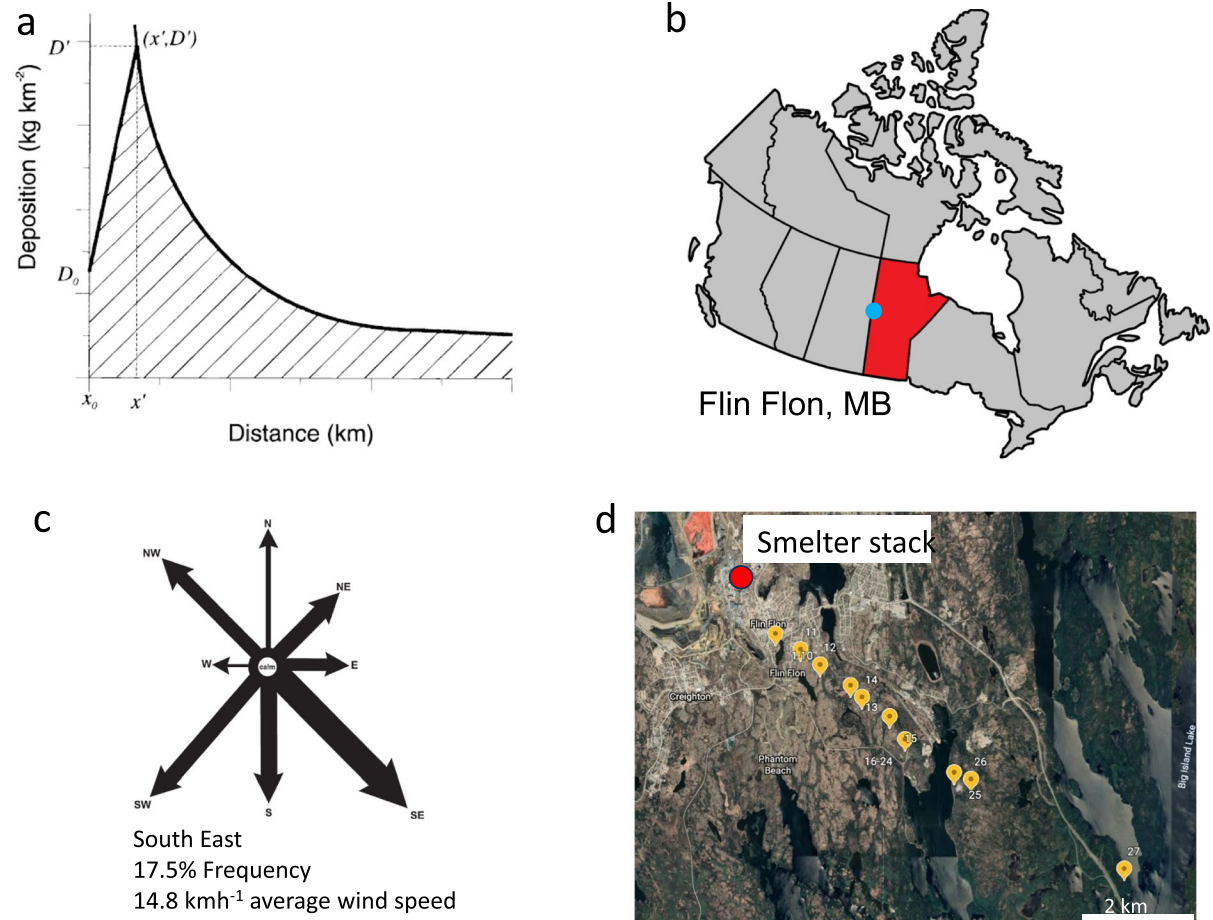


Fig. 1 Smelter-shadow and sampling area (a) the smelter-shadow effect: distance in kilometer from the smelter versus deposition of particulate matter (PM) in kg km^{-2} ; (b) Map of Canada indicating the location of Flin Flon (blue spot) within Manitoba (red coloured); (c) Prevailing wind directions in Flin Flon, Manitoba from 1927-1990; arrow lengths represent

frequency of wind blowing in that direction, arrow widths represent average wind speed; modified from McMartin et al. (1999), data from Environment Canada (1993); (d) satellite image indicating the location of the sampling sites along a NW-SE transect

Lanteigne et al., 2012; Mantha et al., 2019). During this process, PM weathers and its constituents leach into the deeper part of the soil as ions or as a component of the colloidal fraction (Jadoon & Schindler, 2022; Mantha et al., 2019; Schindler et al., 2022; Sterckeman et al., 2000). Among many factors, the weathering of deposited PM is predominantly controlled by climatic conditions, the physical and chemical properties of a soil, the type and solubility of emitted PM and the degree of acidification and neutralization potential of the soil (Bataillard et al., 2003; Carrillo-González et al., 2006; Ettler et al., 2008; Koptsik, 2014; Lanteigne et al., 2014; Lanteigne et al., 2012; Schindler et al., 2016).

Remediation efforts applied to smelter-affected landscapes have the overarching goals of reducing the mobility and bioavailability of metals (e.g., free Al, Zn, Cu and Pb) by fixing them into adsorption complexes, less-soluble compounds, and plant material (Koptsik, 2014). A key example of where a successful chemical and phyto-remediation of acidic metal(loid)-rich soils has been carried out is in the vicinity of the smelter centers in Sudbury, Ontario, Canada (Winterhalder, 1995, 1996; Wren, 2012). Remediation efforts have included liming and fertilization, followed by sowing of a grass–legume mixture (Winterhalder, 1995). Similar remediation efforts like these have resulted in the worldwide reduction of (semi-) barren landscapes and a general decrease in soil acidity and metal mobility (Koptsik, 2014).

This study compares the mobilities of metals between pedons of a remediated (limed) and non-remediated site at the smelter-impacted area of Flin Flon, Manitoba, Canada. It shows that the mobility of some of the emitted metals can be still higher in a pedon of a remediated than non-remediated site as the mineralogical composition of the soils and the average solubility of the PM deposited at these sites have a greater effect on metal mobility than soil pH.

1.1 Previous Studies in the Smelter-impacted Area of Flin Flon, Manitoba, Canada

The town of Flin Flon is located along the Manitoba-Saskatchewan border, in western Canada (Fig. 1b). Here, Au-Cu-Zn ore veins were discovered in 1913-1915 and mining of predominantly Zn commenced in 1930 (Mochoruk, 2004). Early smelter emissions were released by two short stacks and averaged 7150 tons/year of PM between 1940 and 1974. These emissions were reduced to approximately 6834 tons/year with the construction of a single, taller stack in 1974 (McMartin et al., 1999). Emissions were reduced by over 90% to 632 tons/year in 1995 and remained constant until the closure of the smelter in 2010 (Eckley et al., 2015; Intrinsik, 2010; McMartin et al., 1999).

The smelter emission consisted predominantly of Zn, Fe, and Pb, with lesser quantities of As, Cu, Cd, and Hg, and trace amounts of Ag, Al, Mg, Mn, Se, Sb, Ni, Cr, and Co (Henderson et al. 1998 and McMartin et al. 1999). The ratios between the total emissions of the elements [in tons] remain relatively constant over time with for example Zn : Cu ratios of 18.3 and 17.5 during the time spans of 1931-1974 and 1975-1995, respectively (Table 1). Chemical analyses of retained smelter dust in the smelter baghouse and in the Cu and Zn precipitators indicated the occurrence of fine to medium silt size range (2–31 μm) particulates predominantly composed of Cu, Zn, Fe and S with traces of Pb, As, and Cd (Henderson et al., 1998; McMartin et al., 1999).

The impact of the smelter emissions on local lakes and fish populations were first investigated by (Loon & Beamish, 1977), (McFarlane and Franzin, 1978) and (McFarlane & Franzin, 1980). (Franzin et al., 1979) quantified the total metal-deposition on the surficial soils and (Outridge et al., 2011) observed the partial drainage of the metal(loid)s from the soils to the local watershed during spring

Table 1 Total emissions in tons [t] of the metal(loid)s Zn, Pb, Cu and As by the smelter in Flin Flon, Manitoba, Canada during the time spans of 1931-1974 and 1975-1995

metal emissions [t]*	Zn	Pb	Cu	As	Zn : Pb ratio	Zn : Cu ratio	Zn : As ratio
1931-1974	88505	15826	4827	2783	5.6	18.3	31.8
1975-1995	42229	7431	2409	1284	5.7	17.5	32.9

* data from McMartin et al. 1999

snowmelt. Furthermore, (Zoltai, 1988) characterized the distribution of metals in peat bogs around the smelter and (Percival & Outridge, 2013) investigated the mobility of Zn, Cu, Pb, As, and Cd in lake sediments. (Henderson & McMartin, 1995) and (McMartin et al., 1999) studied the spatial distribution of the emitted metal(loid)s in soils with distance to the smelter and with depth at various sites. These studies showed an exponential decrease in the concentrations of As, Cd, Cu, Pb and Zn with distance to the smelter, whereby the volatile elements Hg, As, Cd and Pb were transported farther in air than Zn, and Cu before being deposited (Henderson et al., 1998; McMartin et al., 1999). They further showed that the smelter-emitted metalloids were accumulated in the upper humus-rich layers of the surficial soils in which they occurred above background levels to average distances of 70 to 104 km from the smelter.

The speciation of Zn in organic-rich soils around the smelter was characterized using Scanning Electron Microscopy (Henderson & McMartin, 1995), X-ray absorption spectroscopy and X-ray fluorescence mapping (Hamilton et al., 2016). These studies showed that franklinite, a Zn-spinel ($ZnFe_2O_4$) is the most common Zn-bearing phase in the surficial soils and that Zn is predominantly sorbed to Fe- and Mn-oxides. As the smelter was one of the largest emitters of Mercury (Hg) in North America (Environment Canada National Pollution Release Inventory), the distribution of Hg in humus surficial- and lake-sediments and its emission before and after the smelter closure were studied by (Henderson et al., 1998) (Eckley et al., 2015) and (Wiklund et al., 2017).

1.2 Detailed Objectives

Previous studies focused on the metal(loid) concentrations in soils with distance to the smelter and on the overall dimensions of the smelter impact zone (Henderson et al., 1998; McMartin et al., 1999). As these studies used large sampling intervals ranging from 2 km to over 4 km, they could not resolve any smelter-shadow effect and its impact on the deposition of different types of PM. Furthermore, pedons collected in these studies were sampled in 10–50 cm intervals and only in non-remediated soils outside of the smelter shadow (Henderson et al., 1998; McMartin et al., 1999).

The identification of a smelter-shadow effect, its influence on the deposition of metal(loid)s and the effect of types of emitted PM on the mobility of metal(loid)s such as Zn, Cu, As and Pb requires high-resolution sampling and characterization of surficial soils ranging from 500 m intervals along a transect, to 1.5–5 cm in pedons and to the micrometer-scale at the individual soil grain level. The detailed objectives of this multi-scale study are to investigate whether:

- I. a smelter-shadow effect occurred around the former Zn-smelter in Flin Flon Manitoba, Canada (Fig. 1a);
- II. the mobility and sequestration of Zn, Cu, Pb, and As in soils at a remediated and non-remediated site inside and outside the smelter shadow are different, respectively.

The data gained from these characterizations will be subsequently used to evaluate whether different types of PM deposited on surficial soils within and outside the smelter shadow affected the mobility of elements in the surficial soils.

2 Experimental

2.1 Sampling

High-resolution samplings of surficial soils were conducted along a transect of 5.5 km, with two detailed pedons being sampled in small defined depth increments. The transect followed the prevailing NW-SE winds and thus the reported highest concentrations of metal(loid)s in the soils around Flin Flon (Fig. 1c; (Zoltai, 1988), (McMartin et al., 1999; Percival & Outridge, 2013)). Starting at a distance of one km from the smelter stack (due to the private property around the smelter), nine surficial samples were taken along a transect at 500 m (± 80 m) intervals (Fig. 1d). Sampling sites were in smaller or larger depressions on the bedrock of the Canadian shield (Fig. 1d). In addition, one sample was taken approximately 3 km further down the transect from the penultimate sample to determine the extent to which trends in contaminant distribution continue along the transect (Fig. 1d). Surficial samples were collected with a spade to a depth of 5 cm. Pedons were taken at the first and seventh sampling site at distances of about

1 and 4 km from the smelter stack. These sampling sites are characterized by a large depression in a forest and a small depression on top of a bedrock plateau, respectively. Pedons were collected to a depth of 30 cm (note that the bedrock occurred at 28 cm depth in the second pedon), in 1.5 cm increments for the first five samples and 5 cm for the subsequent samples. Samples were transported in sealed containers to the University of Manitoba, dried at 80°C for 72 hours, and subsequently stored under dry conditions.

2.2 Sample Preparation and Analysis

2.2.1 Bulk Soil Analysis

Soil pH was measured on the field-moist soil samples at the University of Manitoba Environmental Nano Geoscience facility within 24 hours of sample collection. Two grams of sample were mixed with either 10 mL deionized Milli-Q® water or a 0.01 mol/L CaCl₂ solution. Samples were agitated for 20 minutes, allowed to settle for an additional 20 minutes, with soil pH being measured using a Fisher Scientific Accumet Basic AB15 pH meter, calibrated using buffer solutions with pH 4.00, 7.00 and 10.00.

The samples were sent for bulk geochemical analysis to the ALS Labs in Vancouver, BC, Canada. Samples were digested using a four-acid digestion and analyzed by inductively coupled plasma atomic emission spectroscopy (ICP-AES). Quality control included certified reference materials, duplicates and blanks which were analyzed after every tenth sample.

The total carbon content was determined by combustion in an induction furnace at 1000 °C, with infrared quantification of evolved carbon dioxide. The organic carbon content was determined through dissolution of inorganic carbon compounds using a 25% HCl solution, followed by quantification the organic residue using the induction furnace. The inorganic carbon content was calculated by the difference between the total carbon and the organic carbon content. The results of these analyses are listed in the supplementary data S1.

2.2.2 Leaching of the Surficial Horizons in the Pedons with Simulated Rainwater

Leachates of the surficial soil samples in the pedons 1 and 2 were collected in flow-through experiments

using hollow plastic tubes. Prior to both runs, the tubes were rinsed with ethanol and ultrapure water. The tubes were subsequently filled with 3 cm of 3 mm diameter plastic, followed by 5 cm of dried soil samples.

A 0.02 mM CaCl₂ solution (ionic strength = 6×10^{-5}), simulating the ionic strength (I) of rainwater (I ~ lower 10^{-5} range Salve et al., 2008), was passed through the column at an approximate rate of 0.8 mL h⁻¹ until 50 mL was collected in a flask below the column. The leachates were subsequently filtered with a 20 nm filter in order to separate the majority of the colloids from the true dissolved fraction. Unfiltered samples were digested with nitric and hydrochloric acids to dissolve the colloidal fraction. Filtered samples were preserved with addition of 0.3 ml ultrapure nitric acid. Total metal concentrations of the filtered and unfiltered samples, together with duplicates and blanks, were analyzed by ICP-MS at ALS Winnipeg. The results of these analyses are listed in Table S2.

2.2.3 Powder X-Ray Diffraction

A small handheld magnet was used to yield fractions of selected soil samples enriched in sulfides and Fe-bearing spinels relative to quartz. These fractions were ground with an agate mortar and pestle to an average grain size of 20 µm for analysis with a Siemens D5000 Diffractometer using a current and voltage of 40 mA and 40 kV, respectively. X-ray powder diffraction patterns were recorded over a 2θ range of 5–60° with a step size of 0.02° and a dwell time of 1 s., Phase identification was conducted with the software Crystallographica Search-Match. All diffractograms are shown in the supplementary data S3.

2.2.4 Scanning Electron Microscopy

Surficial soil material from 0–1.5 and 1.5–3 cm depth from the pedons 1 and 2 and from 0–5 cm at 3.7 km from the smelter stack were embedded into epoxy pucks and prepared for SEM examination using an FEI Quanta FEG 650 SEM using an accelerating voltage of 15 kV and a beam current of 1 nA. Soil grains and organic particles were analyzed in both backscatter and secondary electron mode, with elemental distributions being recorded with the TEAMS SEM-EDS software. The chemical compositions of areas and points were determined

semi-quantitatively using the ZAF method (*i.e.* no external standards were used).

2.2.5 Identifications of the Soils and Grain Size Distribution

The identification and the grain size distribution of the surficial soil samples at depths of $D = 1.5\text{--}3\text{ cm}$ and $4.5\text{--}6\text{ cm}$ at both pedons were determined using the Canadian Foundation Engineering Manual, 3rd Edition and using the American Society for Testing and Materials standard sieves with the mesh openings of 4 mm, 2 mm, 1.4 mm, 1 mm, 425 μm , 355 μm , 250 μm , 125 μm , 75 μm and 63 μm . The plots are shown in supplementary data S3.

3 Results

The surficial soils (0–5 cm) along the transect are gray/dark gray (10R 6/1, 10R 6/2, 10R 4/1) to very dark grayish brown (10R 3/2) near the smelter (< 6

km) and dark/very dark greyish brown (10R 4/2, 10R 3/2) to very dark brown (10R 2/2) towards end of transect (6–9 km from the smelter). The soil materials are mainly composed of quartz and minerals of the feldspar and plagioclase group with minor amounts of chlorite-, clay- and spinel-group minerals. The soils are acidic with pH values varying between pH 3.5 and 5.0. The pH values are higher closer and farther away from the smelter with a minimum of pH 3.7 at around 4 km (CaCl_2) from the smelter stack (Fig. 2a). The total concentrations of (Ca+Mg) depict a similar trend with distance to the smelter. Here, higher concentrations occur closer and farther from the smelter with a minimum between 3 and 4 km from the smelter (Fig. 2b).

The major contaminants Zn, Cu, As and Pb display opposite trends to the observed pH and (Ca+Mg) concentrations. Their change in concentration (in the upper 5 cm) with distance to the smelter shows a typical profile for a smelter-shadow effect with lower concentrations closer and farther away from the smelter (Fig. 2c–f). However, the locations of their maximum

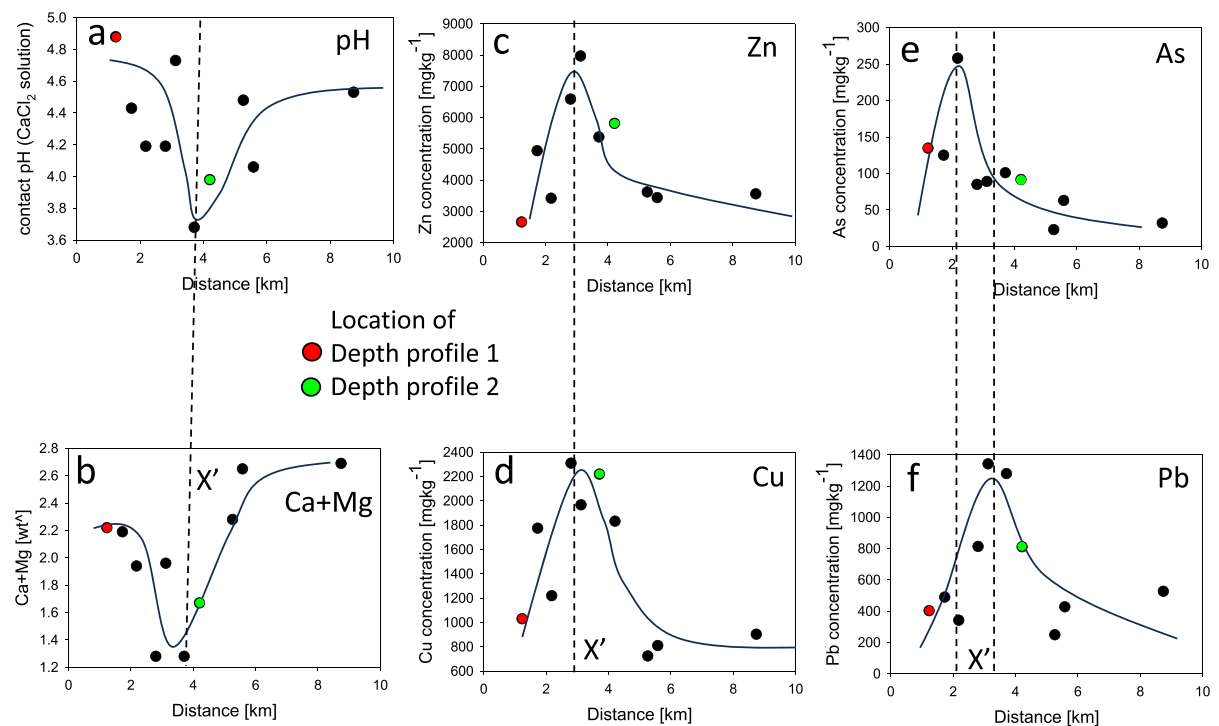


Fig. 2 Contact pH and distribution of elements along the transect with distance to the smelter. (a) contact pH value, (b) the sum of the concentrations of Ca and Mg; (c) Zn, (d) Cu, (e) As

and (f) Pb; the locations of the pedons 1 and 2 are indicated with a red and green-coloured circle, respectively

concentrations differ as the peak concentration for (a) As occurs at ~2 km, (b) Zn at ~3 km and (c) Cu and Pb at ~3.5 km (Fig. 2c-f). Note that these plots display the average concentrations of As, Cu, Pb and Zn in the upper three layers (0-1.5, 1.5-3 and 3-4.5 cm) of the pedons at 1 and 4 km from the smelter.

3.1 Textural and Chemical Features in the Pedons 1 and 2

The soils in pedon 1 depict characteristic features of a Humic Luvic Gleysol soil overlying till. These grayish-dull soils are highly compact and are common in the glacial landforms of Northern Manitoba and Saskatchewan (Lavkulich & Arocena, 2011) (Fig. 3a). The soil samples are sand with minor gravel and silts and with a mean diameter of 0.66 and 0.93 mm for the 1.5-3.0 cm and 4.5-6.0 cm depth increments samples, respectively. The organic C content is

higher in the surface LFH horizon (29.8 wt%) than in the underlying Ahg horizon with a relatively constant organic C content (13 to 15 wt%) to D = 6.75 cm.

The sandy soils in pedon 2 show features characteristic of an eluviated Dystric Brunisol soil (CSSC, 1995) with a bleached Ae horizon in greyish tones (10R 6/1) followed by a light- to reddish-brown B horizon (7.5R 7/6) (Sanborn et al., 2011) (Fig. 3b). The soils samples are gravelly sands with traces of silt (sand in the less than 2 mm fraction). Below a depth of circa 4.5 cm, the horizon samples contain minor amounts of clay minerals (XRD, supplementary data S3). The textural data for the samples at D = 1.5-3 cm and 4.5-6.0 cm indicates mean grain sizes of 1.05 mm and 1.25 mm, respectively. The organic carbon content decreases exponentially with depth from 27.7 wt% in the surface layer to 1 wt% at D = 6.5 cm.

The sampled pedons show different trends in pH and (Ca+Mg) concentration with depth. The pH

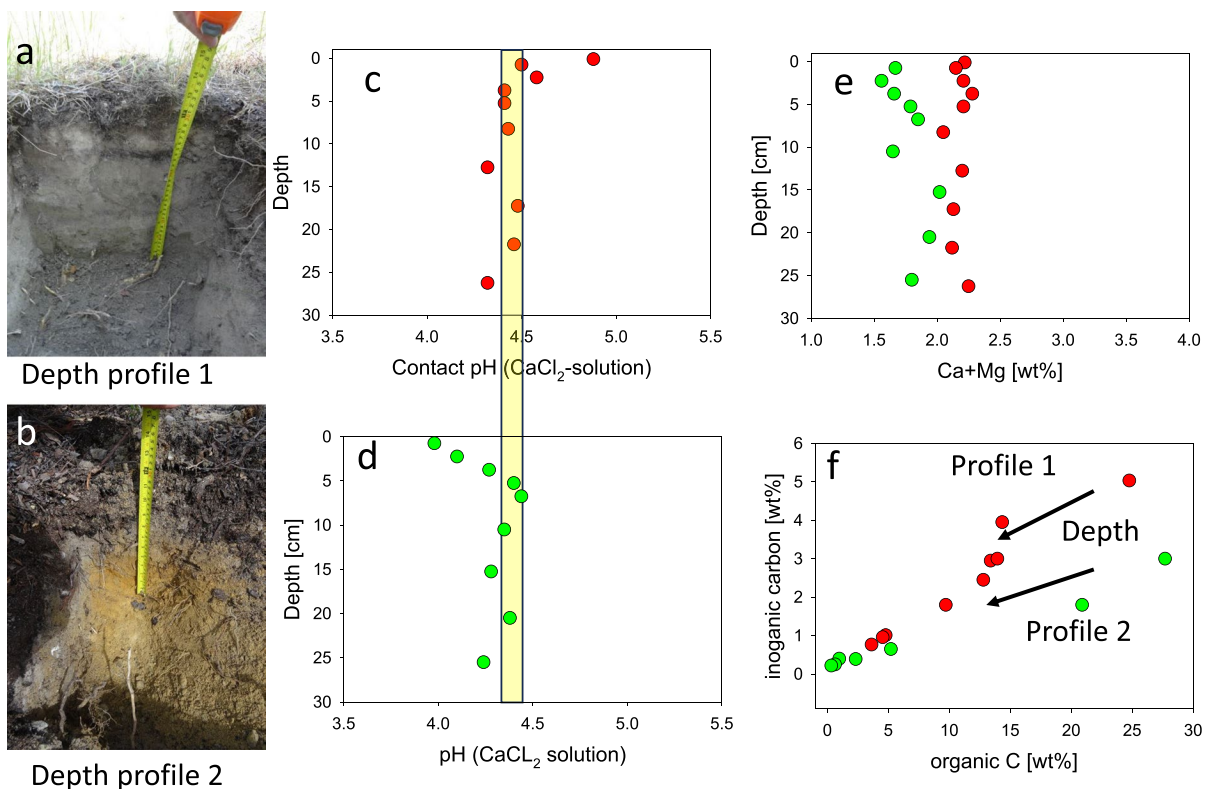


Fig. 3 (a)-(b) photographic images of the pedons 1 and 2; (c)-(d) change in contact pH-value with depth (measured with a CaCl₂ solution); (e) comparison of the distribution of the sum of Ca and Mg (in [wt%]) with depths in the pedon 1

(red spheres) and 2 (green spheres); (f) plot of the amount of organic versus inorganic carbon (in wt%) in the surficial horizons of pedon 1 (red spheres) and 2 (green spheres) (arrows indicate the corresponding changes in depth)

values of the surficial horizons in pedon 1 are pH = 4.5-5.0, whereas those in pedon 2 depict pH values of pH = 4.0-4.5. However, soil layers at greater depths in pedon 1 and 2 show similar pH values, in the range of pH = 4.2-4.5 (Fig. 3c and d). Furthermore, all soil horizon layers in pedon 1 depict (Ca+Mg) concentrations in the range of 2.0 to 2.3 wt%, whereas those in pedon 2 have (Ca+Mg) concentrations of 1.5-2.0 wt% (Fig. 3e). A plot of the concentrations of organic versus inorganic carbon of the soils in the upper parts of pedon 1 (D = 0-7.5 cm) and pedon 2 (D=0-18 cm) indicates that the top layers of pedon 1 have much higher proportions of inorganic versus organic carbon (Fig. 3f).

The distribution of Fe and Al in the two pedons appear to be linked with the changes in pH. In pedon 1, maximum concentrations of Fe occur below the surficial layer (D = 0-1.5 cm) at the rising limb of an increasing soil pH (Fig. 4a, b). At the same depth, the concentrations of Al slightly increase and remain relatively constant beneath these layers (Fig. 4c).

In pedon 2, the concentrations of Fe are on average much lower than in pedon 1. They depict minimum and maximum concentration below the surface (D = 1.5 – 3cm) and in the layer directly beneath the more acidic surficial horizons (D = 5cm), respectively (Fig. 5b, d). The concentrations of Al are lowest in the surficial horizons and increase with depth until D > 7.5 cm where they depict similar values to those of pedon 1.

The distribution of As, Cu, Pb and Zn in pedon 1 are characterized by lower concentrations in the surface layer (0-1.5 cm) and maximum concentrations in the layer beneath (1.5-3 cm) (Fig. 5). The decline in concentration with depth (D) is relative sharp for As, Pb and Cu with background concentrations occurring at D ~ 15 cm (Fig. 5b, c and d), whereas the concentrations for Zn reach background levels at or below the bottom of the pedon (Fig. 5a). Conversely, the concentrations of As, Cu, Pb and Zn display maxima at the surface layer (D = 0-1.5 cm) of pedon 2 (Fig. 6). They decrease exponentially to background

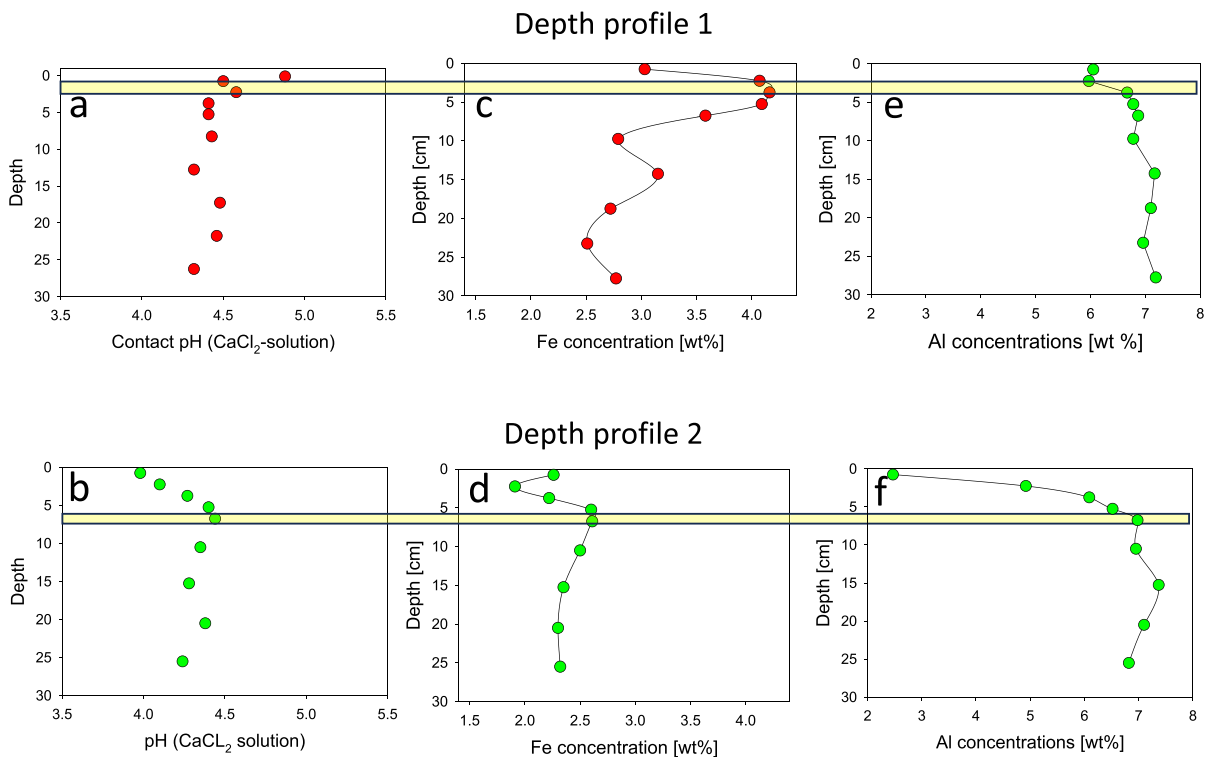


Fig. 4 Comparison of the contact pH value with the distribution of Fe and Al with depth in the pedons 1 (red spheres) and 2 (green spheres); (a)-(b) contact pH value; (c)-(d) concentra-

tion of Fe (in [wt%]) with depth; (e)-(f) concentrations of Al (in [wt%]) with depth

Depth profile 1

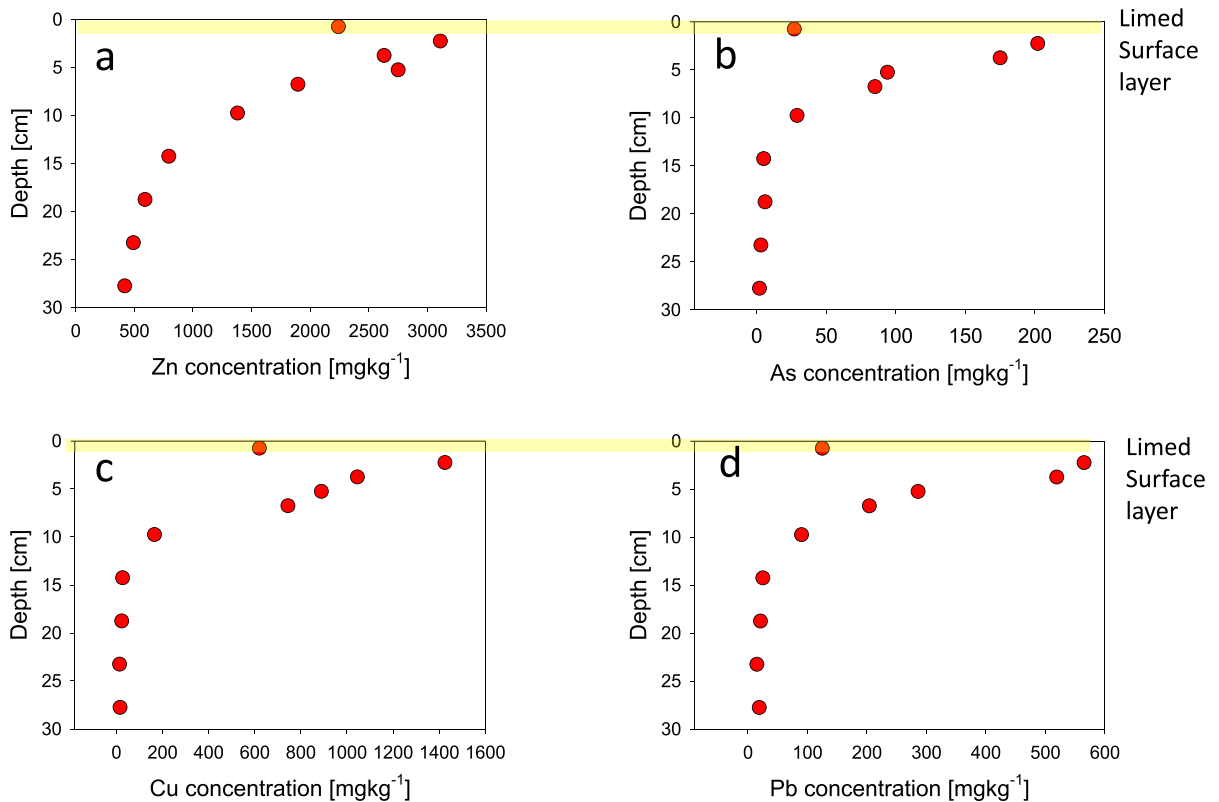


Fig. 5 Distribution of selected elements in pedon 1 with depth (a) Zn, (b) As, (c) Cu and (d) Pb (all in mg kg⁻¹); the location of what appears to be a limed surface layer is shaded in yellow

levels for Cu, Pb and Zn at ~ 7 cm (Fig. 6a, c and d), whereas the concentrations for As never reach background levels (Fig. 6b). Note that a background concentration of an element is defined here as the relative constant concentration range at greater depth.

3.2 Mineralogical Features in the Surficial Horizons of the Pedons 1 and 2

In the surficial horizons of both pedons and in the surficial layer at 3.7 km from the smelter (located between the peak of deposition and pedon 2), the predominant Zn-bearing phase (observable with SEM) is franklinite ZnFe_2O_4 . The phase occurs in smelter-derived spherical particulates (Fig. 7a and b) and as lens-shaped precipitates in pore spaces of organic matter (OM) (Fig. 7c-d) and as blocky submicron crystals in mineral surface coatings on Fe-hydr(oxide)

grains (Fig. 7e-f). Another prominent Zn-phase is ZnS (sphalerite or wurtzite), which occurs in the core of smelter-derived spherical particles (Fig. 7a-b) or as lens-shaped precipitates in organic matter (Fig. 7c-d). The ratio of Zn-bearing spinels versus Zn-sulfides is circa 5:1 in the surficial soils of both pedons (Fig. 8a and b).

Identified phases containing Cu as a major element include chalcopyrite and cuprospinel with both occurring in spherical smelter-derived particulates. Copper is also a minor element in franklinite and Fe-(hydr)oxide precipitates (Fig. 8b). Lead- and As-bearing phases were not identified with SEM.

The abundances of spinels in the surficial soils of the two pedons may be recognized on the area ratios (spinel A / quartz A) between the 100% peaks for spinel ((311) at $d=2.4\text{--}2.6 \text{ \AA}$) and low quartz ((011)/(101) at $d = 3.3\text{--}3.4 \text{ \AA}$) in the corresponding

Depth profile 2

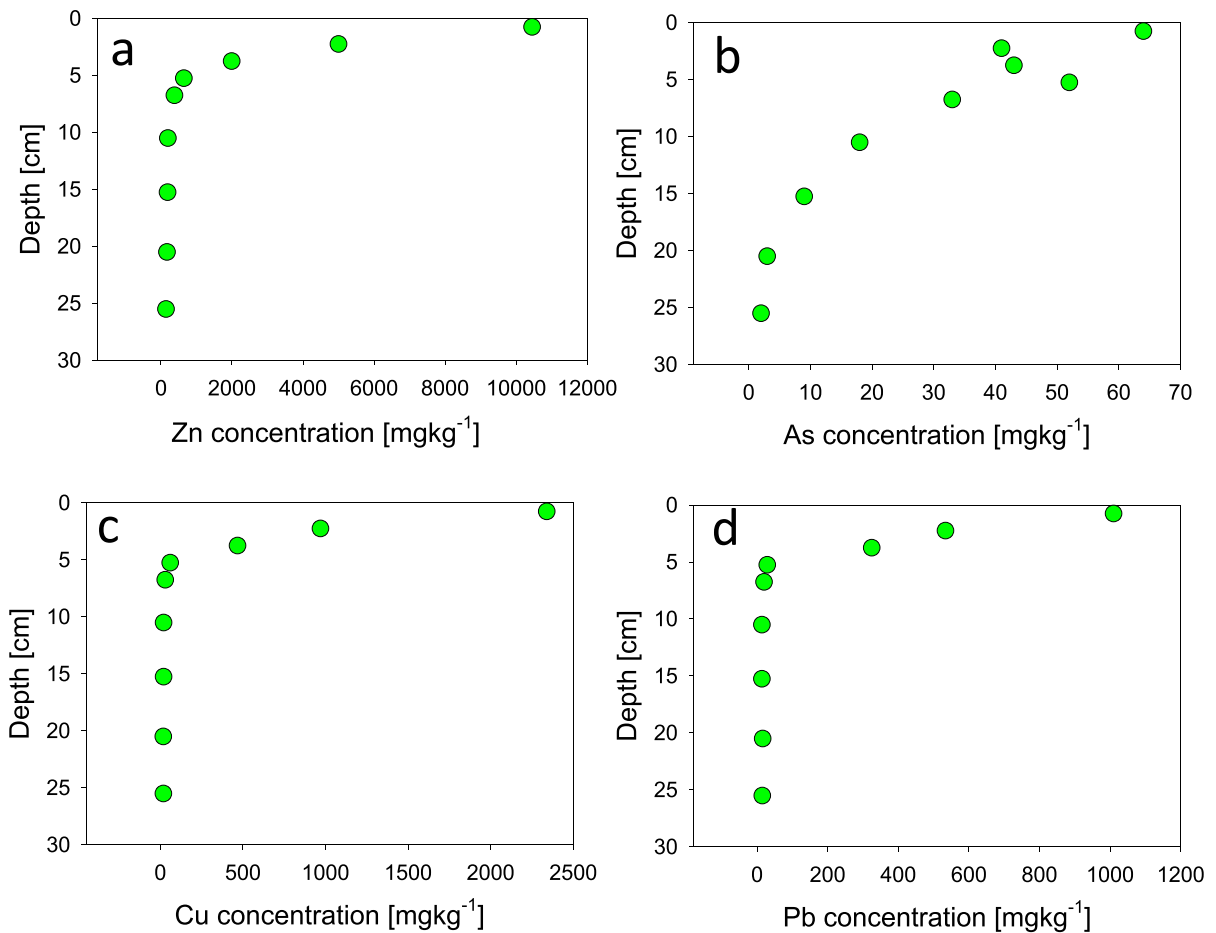


Fig. 6 Distribution of selected elements in pedon 2 with depth (a) Zn, (b) As, (c) Cu and (d) Pb (all in mg kg⁻¹)

powder X-ray diffraction pattern. The areas of these two peaks were estimated assuming a peak shape defined by a 1 : 1 ratio of a Gaussian and Lorentzian distribution with areas of $A = 1.06 * h * w$ and $A = \pi * h * w$ (h = height of peak and w = full width at half maximum), respectively. Here, the ratios spinel A / quartz A of 0.02, 0.08 and 0.44 for the surficial horizons of pedon 1 ($D= 0-1.5$ cm and $1.5-3.0$ cm) and 2 ($0-1.5$ cm) indicate a higher abundance of spinels in the latter than former surficial horizons, respectively.

3.3 Chemical Compositions of the Leachates

Through the Surficial Horizons of Pedons 1 and 2

Leaching experiments were conducted using the surficial samples with the highest concentrations of metal(loid)s (samples at $D = 1-5-3$ cm and $D = 0-1.5$ cm in pedons 1 and 2, respectively). As the concentration of an element in a leachate (C_{liquid}) depends foremost on its concentration in the solid (C_{solid}), one can define a leaching factor as the concentration ratio between C_{liquid} and C_{solid} in

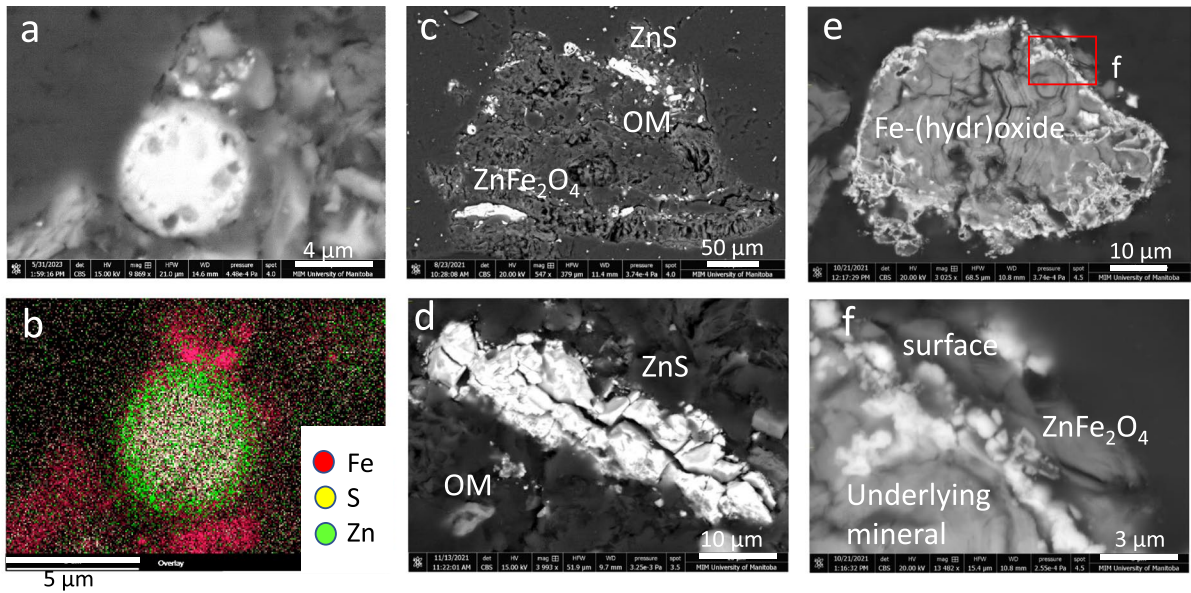


Fig. 7 Various types of abundances of franklinite (identified on the basis of a Zn : Fe ratio of 1:2) and ZnS (either sphalerite or wurtzite) (a) SEM image in BSE mode and chemical distribution map of Fe (in red), S (in yellow) and Zn (in green) of a spherical particulate containing ZnS in the core and franklinite

in the rim; (c)-(d) precipitates of ZnS and ZnFe₂O₄ in organic matter; (e)-(f) mineral surface coating on a Fe-(hydr)oxide grain containing submicron franklinite particles; the location of the image shown in (f) is indicated with a red square in (e)

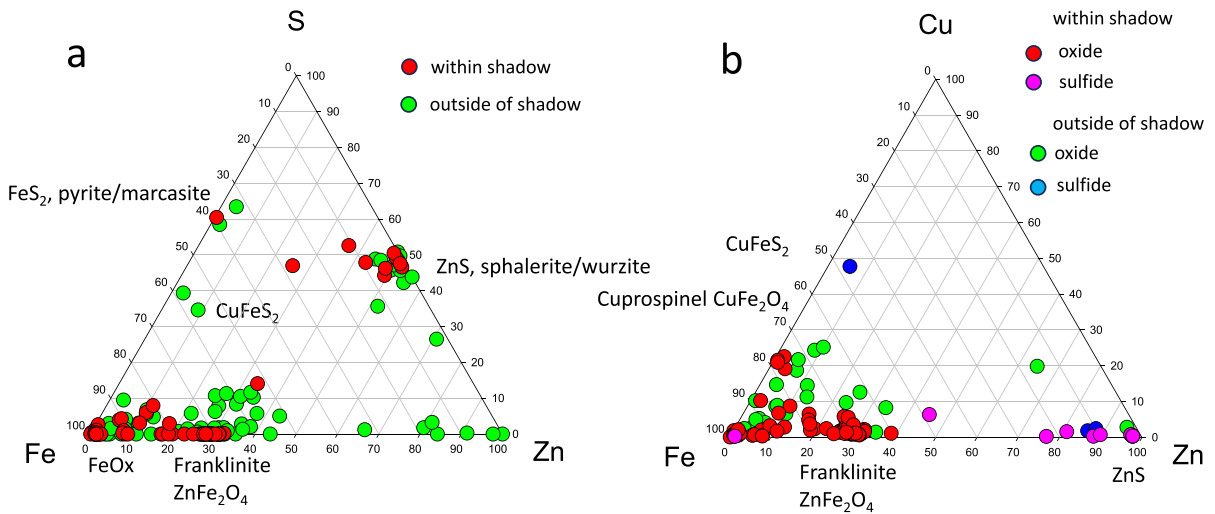


Fig. 8 (a)-(b) triangular diagrams depicting the proportion of (a) Fe, Zn and S and (b) Fe, Zn and Cu in Zn- or Cu-bearing soil components such as spherical particulates, precipitates in organic matter or mineral surface coatings; red and green

spheres indicate in (a) components within and outside the smelter shadow; in (b) red and green as well as pink and blue spheres indicate oxides and sulfides within and outside the smelter shadow, respectively

permille notation (*1000). The leaching factors for the selected elements As, Cu, Fe, Pb and Zn in the surficial horizons of pedons 1 and 2 indicate that

with the exception of As, the concentration ratios are higher for Cu, Fe, Pb and Zn in the surficial horizons of pedon 1 than 2 (Table 2). Furthermore,

Table 2 Ratios between the concentrations of selected elements in the leachate (C_{liquid}) and their concentrations in surficial horizons of pedons 1 and 2 (C_{solid}) and their percentages in the colloidal fractions ($D > 20$ nm) of the leachates

Element	Pedon 1, D=1.5-3 cm			Pedon 2, D=0-1.5 cm		
	$C_{\text{liquid}}/C_{\text{solid}} * 1000$		%colloidal	$C_{\text{liquid}}/C_{\text{solid}} * 1000$		%colloidal
	D>20 nm	D<20 nm		D>20 nm	D<20 nm	
As	1.4	1.3	6	3.5	3.3	6
Cu	2.9	2.6	11	0.5	0.44	11
Fe	0.06	0.05	14	0.03	0.03	25
Pb	0.08	0.04	23	0.06	0.02	44
Zn	1.4	1.4	1	0.8	0.8	6

the leaching factors are generally larger for Cu and Zn than for the less mobile Fe and Pb. The proportion of an element in the colloidal fraction of the unfiltered sample (% colloidal) may be calculated through subtracting its concentration in the filtered ($D < 20$ nm) from the unfiltered solutions. Table 2 indicates that the proportions of the elements in the colloidal fractions of both leachates increase in the sequence $Zn \leq As < Cu < Fe < Pb$.

4 Discussion

Previous geochemical studies, including a large-scale study by the Geological Survey of Canada and Manitoba Energy and Mines (1600 sites within a 200 km radius of the stack in Flin Flon, Manitoba) resolved two-dimensional distribution pattern of the major contaminants around the smelter in Flin Flon (Henderson et al., 1998; McMartin et al., 1999). Due to the smaller sampling interval closer to the smelter, this study resolves a smelter-shadow effect for the major contaminants As, Cu, Pb and Zn in the surficial soils along a NW-SE transect. Furthermore, the occurrence of distinct distribution patterns for As, Cu, Pb and Zn in two pedons, one within and one outside the smelter shadow, is resolved. We will first discuss mineralogical and chemical features in the surficial soils along the transect and within the pedons before addressing whether the observed distribution pattern of As, Cu, Pb and Zn in the pedons are related to (a) textural, mineralogical and geochemical properties of the soils or (b) the type of PM deposited within and outside the smelter shadow.

4.1 Mineralogical and Chemical Features in the Surficial Soils Along the Transect

Previous studies on the environmental impact of smelters showed that larger emitted particulates occur as spherical particulates (the industrial term is prills) in soils, snow, and rock coatings (Ettler et al., 2008; Gregurek et al., 1999; Gregurek et al., 1998; Knight & Henderson, 2006; Lanteigne et al., 2012). These particulates form at high T during smelting and converter processes and possess distinct internal and external features as a result of their rapid cooling (Knight and Henderson 2005, 2006). They are commonly composed of Fe-silicates and Ni-Cu-Zn-Fe-oxides with minor Fe-Ni-Cu-Zn-sulfides. The type of sulfide and spinel depends mainly on the type of ore with Cu-Ni-Fe-oxides and -sulfides dominant around the Cu and Ni smelters in Sudbury, Ontario, Canada whereas Cu-Zn-Fe-oxides and -sulfides are predominant around the smelters in Flin Flon, Manitoba, Canada and Rouyn-Noranda, Quebec, Canada (this study; (Knight & Henderson, 2003) (Knight & Henderson, 2006); Fig. 7a and b). In addition to spinel and sulfides, the spherical particulates also exhibit a prominent rim containing the more volatile elements Pb and As, which attach to the particulates at a later stage in the smelter or converter (Lanteigne et al., 2014; Lanteigne et al., 2012). Although nanometer-size spherical particulates were identified in rock coatings, the majority of spherical particulates in smelter-impacted soils are in the micrometer-size range (Lanteigne et al., 2014).

In addition to previous soil studies in the Flin Flon area which identified spinels as the major hosts for Zn (Henderson et al., 1998) (Hamilton et al., 2016), this

study showed that (a) secondary franklinite as well as Zn-sulfides (either wurtzite or sphalerite) occur as lens-shaped precipitates in pore spaces of organic matter and as submicron blocky crystals in mineral surface coatings (only franklinite; Fig. 7c, e and f) and (b) the proportion of spinels relative to quartz in two surficial soils correlate with their Zn concentrations. These observations indicate that secondary spinels and sulfides formed at low-T are major sinks for Zn in these soils, in accord with previous mineralogical studies on soils and tailings, which showed that spinels (other than magnetite) can indeed form in low-T environments and sequester elements such as Pb, Sb, Cu, Zn and Ni (Jadoon & Schindler, 2022; Jadoon et al., 2022; Mantha et al., 2019). The underlying mechanisms for the formation of secondary Zn-sulfides and franklinite within organic-rich soils at Flin Flon will be addressed elsewhere.

4.2 Chemical Features of the Soils in the Two Pedons

The soils of the two pedons represent characteristic soils of the Flin Flon area: the gray Humic Luvic Gleysol of pedon 1 formed in tills deposited by the Keewatin ice sheet, which are coarse textured, non-calcareous, and naturally enriched in heavy metals when overlying bedrock (Franzin et al., 1979). However, higher pH (Fig. 3a), higher ratios of inorganic to organic carbon (Fig. 3f) and lower concentrations of smelter-emitted metal(loid)s As, Cu, Pb and Zn (Fig. 5) in the surficial LFH horizon of pedon 1 than in the Ahg horizon beneath are in contrast to pedons of acidic smelter-impacted soils in Canada (Nkongolo et al., 2013) and indicate the previous liming of the surficial soils of pedon 1. The liming of the soils likely led to the infiltration of near-neutral pore water and thus in the enrichment of Fe in the Ahg horizon, most likely due to the enhanced precipitation of Fe-(hydr)oxides (Fig. 4c).

The Brunisolic soil of pedon 2 is typical for soils formed under acidic conditions on the Canadian shield, being characterized by a leached Ae layer depleted in Fe and Al and a B horizon enriched in Fe and with constant Al concentrations occurring in the underlying saprolite and bedrock (Fig. 4d and f; Sanborn et al. 2011). The pedon also shows the characteristic of a soil impacted by acidic emissions from

a smelter with surficial soils of greater acidity and higher concentration of metal(loid)s (Fig. 4b and 6).

4.3 Depth Gradients of the Emitted Metal(loid)s in the Two Pedons

The mobility of an element in a soil column depends on the number, duration, intensity, and frequency of precipitation events, the properties of the soils (i.e. pH, total surface area, mineralogical composition, organic matter content, mean grain size and texture), the affinity of the element to sorb on mineral surfaces and organic matter, the speciation of the element (i.e. nanoparticle, colloid, solute), concentrations and types of available colloids, type and abundance of microbial communities, and in the case of atmospheric emissions, on the type of PM deposited on the surficial soils (i.e. its size and solubility) (Bataillard et al., 2003; Carrillo-González et al., 2006; Kretzschmar et al., 1999; McCarthy & Zachara, 1989).

The mobility of As, Cu, Pb and Zn in the two pedons may be estimated from their distribution with depth. Closer inspection of the corresponding plots indicates that the concentrations of the elements decrease exponentially with depth (Figs. 5, 6 and 9a-b), resembling a decay rate of a radiogenic isotope or the diffusion of an element into a solid. As the downward movement of an element depends on the concentration in the surface layer (C_o), we plotted the natural logarithm (\ln) of C/C_o for Cu and As in pedon 2 versus depth, where C is the concentration of the element at depth D (Fig. 9c, d). In the case of Cu, the plot $\ln C/C_o$ vs. D depicts two linear relations with the regression lines 1 and 2 intersecting at a depth where the concentrations of the element reach background level (between $D = 6.75$ and 10.5 cm, Fig. 9a and c). In the case of As, the plot $\ln C/C_o$ vs. D depicts only one linear relation as the concentrations of the element never reach background level (Fig. 9b and d). The linear relations for Cu (regression line 1) and As in the plots $\ln C/C_o$ vs. D can be expressed with the equation

$$\text{Depth} = -m \ln C/C_o + b \quad (1)$$

where $-m$ is the slope (the negative sign indicates that the concentration decreases with depth) and b is the

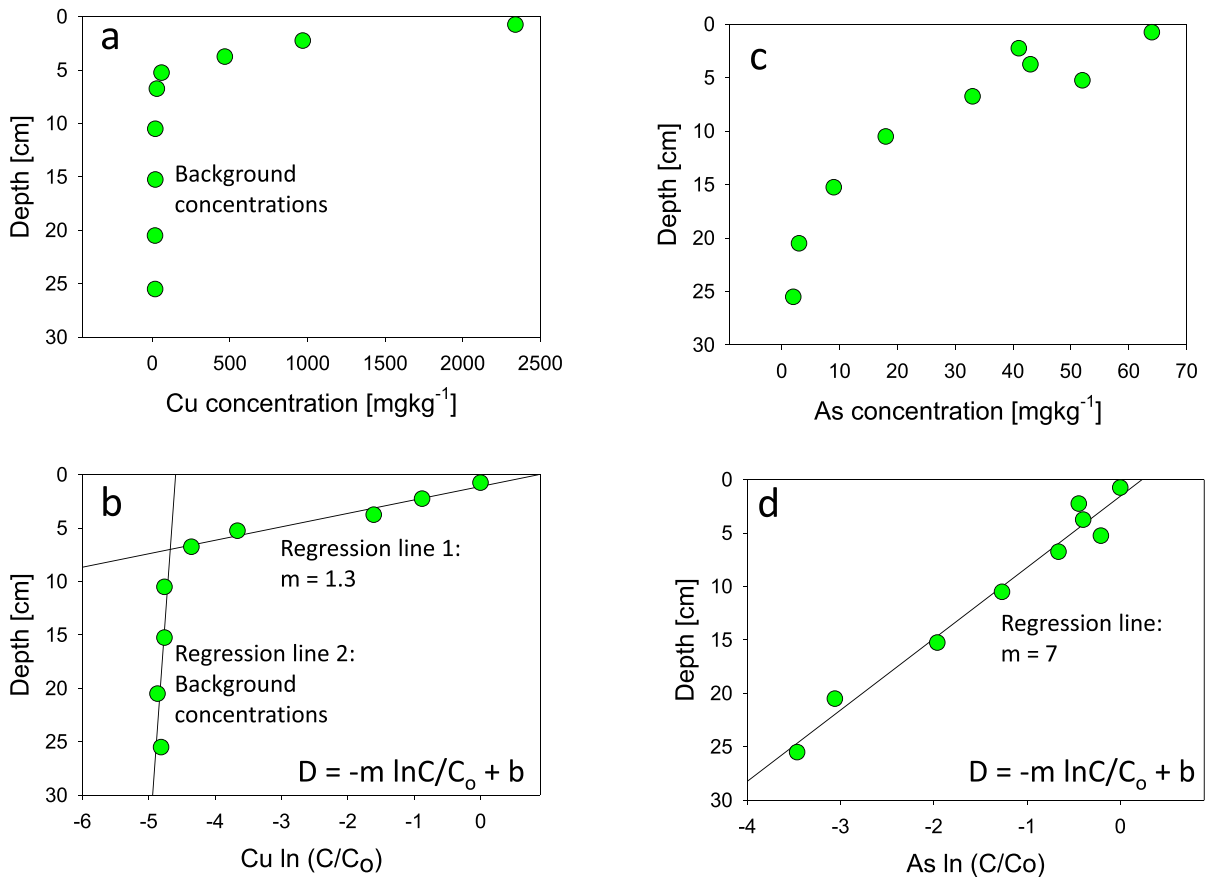


Fig. 9 (a)-(b) distribution of Cu with depth in pedon 2: (a) concentration C and (b) ln C/Co versus depth; (c)-(d) distribution of As versus depth in pedon 2: (c) concentration C and (d)

ln C/Co with depth; Co is the concentration of Cu or As in the surface layer; regression lines and their slopes are indicated in the plots (b) and (d)

intersection with the y-axis. As the latter intersection should be ideally the same for each element, only the slope *m* depicts the change in concentration of an element with depth. We define here the slope *m* as the depth gradient as it expresses the depths (in cm) at which the concentration ratio *C/C₀* of an element decreases by one order of magnitude. In the case of Cu and As, these depth gradients are *m* = 1.3 cm and *m* = 6.7 cm (Fig. 9c and d), indicating that the concentration gradients *C/C₀* decrease by one order of magnitude within 1.3 and 6.7 cm depth for Cu and As, respectively. If we assume, given that the ratios between the total smelter emissions of As, Cu, Pb and Zn remained constant over time (Table 1), that As-, Cu-, Pb- and Zn-bearing PM were deposited simultaneously on the surficial soils and consider that a higher mobile element creates higher *C/C₀* ratios

Table 3 Depth gradients *m* for As, Cu, Pb and Zn in the pedons 1 and 2; the gradients were calculated using linear regression analysis of plots with ln(C/Co) versus depth.

Element	Depth gradient <i>m</i> in pedon 1 [cm]	Depth gradient <i>m</i> in pedon 2 [cm]
Pb	3.8	1.3
As	3.1	6.7
Cu	6.9	1.3
Zn	9.1	2.2

at greater depth, the mobility of As, Cu, Pb and Zn in each pedon should correlate with their respective depth gradients *m*.

Following the same procedure as for Cu and As in pedon 2, the concentration gradients *m* are calculated for As, Cu, Pb and Zn in the pedons 1 and 2

(Table 3), considering hereby that the initial surface layer of pedon 1 occurred at $D = 1.5\text{--}3.0$ cm (Fig. 5). Table 3 indicates that the depth gradients for Cu, Pb and Zn are higher in pedon 1 than 2 (by a factor of 3 or higher) and for As higher in pedon 2 than 1. The depth gradients also indicate that the gradients for Pb are always equal or lower than those for Cu and Zn and that the gradients for Zn are always higher than the ones for Cu. We will first discuss the differences in gradients between the two pedons before addressing differences in depth gradients between the elements within the same pedon.

4.4 Depth Gradients, Leaching Factors, Soil Properties and Type of PM

The observed differences in depth gradients of the elements (Table 3) show the following relations to the mineralogical composition of the surficial horizons and the respective leaching factors of the elements (Table 2):

- (a) lower depth gradients of Cu, Pb and Zn in pedon 2 than 1 (Table 3) coincide with lower leaching factors (Table 2) and with a higher abundance of Cu-Zn-bearing spinels in the surficial horizons of pedon 2 than 1;
- (b) a lower depth gradient of As in the pedon 1 than 2 (Table 3) coincides with a lower leaching factor (Table 2) and a higher amount of Fe (~ 4 wt% vs. ~ 2 wt% Fe; Fig. 4c, d) in the surficial layers of pedon 1 than 2.

Larger depth gradients and leaching factors of Cu, Pb and Zn in pedon 1 than 2 indicate a higher mobility of these elements in the former than latter pedon. As indicated above, the mobility of elements in a pedon depends on numerous factors but the following observations indicate that the type of particulate matter deposited on the surface of the pedons and the mineralogical composition of the surface layers played a more important role than soil pH and soil texture:

I. Soil pH

(Barrow & Whelan, 1998) and (Harter and Naidu, 2001) showed for sandy soils similar to pedons 1 and 2 that a unit increase in pH produced a 2-10-fold increase in the sorption of divalent cations such as Zn^{2+} . Hence, the mobility/leaching of Cu, Pb and Zn

should be lower in the surficial horizons of $\text{pH} = 4.9$ (pedon 1) than in those with a soil pH of $\text{pH} = 3.9$ (pedon 2).

II. Soil texture

The sampling of the soil samples with a spade rather than sample core did not allow the subsequent determination of the change in bulk density or porosity with depth. However, both pedons have sandy organic-rich surficial soil horizons (1.5-6.5 cm for pedon 1 and 0-4.5 cm for pedon 2), where the surficial horizons of pedon 2 depict on average a higher amount of organic matter (19.8 wt% versus 13.5 wt%) and a higher proportion of gravel and thus higher average grain sizes with 1.25 mm (pedon 2) versus 1.05 mm (pedon 1), respectively. As the amount of organic matter, proportion of gravel and average grain size correlate with the infiltration rates (Liu et al., 2018; Rieke-Zapp et al., 2007), one would expect a higher infiltration rate in the surficial horizons of pedon 2 than 1. However, the concentration differences for Cu, Pb and Zn in the above listed depth intervals are much higher for pedon 2 (Cu: from 2340 to 468 mg kg^{-1} ; Pb: from 1010 to 325 mg kg^{-1} ; Zn: from 10450 to 1990 mg kg^{-1}) than for pedon 1 (Cu from 1425 to 889 mg kg^{-1} , Pb from 565 to 286 mg kg^{-1} ; Zn from 3110 to 2750 mg kg^{-1}), suggesting that textural features in the upper surficial horizons had a small effect on the mobility of these elements.

III. Colloidal transport

Previous studies on the colloidal transport of metals in smelter-impacted soils showed that the proportion of the elements Zn, Cu and Pb in the colloidal fractions commonly increased in the sequence $\text{Zn} < \text{Cu} < \text{Pb}$ (Denaix et al., 2001; Jadoon & Schindler, 2022; Jadoon et al., 2022; Sigg et al., 2000). The leaching experiment of the horizons of both pedons showed the same trend with similar proportions of As, Cu, Pb and Zn in the leachates of the samples from pedon 1 and 2 (Table 2). Hence, the proportions of the elements in the colloidal fractions of both leachates do not indicate any major differences in the colloidal transport of As, Cu, Pb and Zn between the surficial horizons of both pedons.

IV. Type of particulate matter

In addition to the aforementioned micrometer-size spherical particulates, smaller particulates predominantly composed of sulfates, arsenates and chlorides are emitted by base-metal smelters. Previous studies

at smelters elsewhere showed that these particles are composed of, among others, CuSO_4 , ZnS , ZnSO_4 , ZnO , $\text{ZnSO}_4 \cdot \text{H}_2\text{O}$, $(\text{Cu}_{0.94}\text{Zn}_{0.06})_2(\text{AsO}_4)(\text{OH})$, As_2O_3 , $(\text{Cu}_{0.84}\text{Zn}_{0.16})(\text{AsO}_3\text{OH})$, $\text{Zn}_3(\text{AsO}_4)_2$, metallic Pb, PbSO_4 , PbS , $\text{PbO} \cdot \text{PbSO}_4$, $4\text{PbO} \cdot \text{PbSO}_4$, PbSO_3 , $(\text{Na}_3\text{Pb}_2(\text{SO}_4)_3\text{Cl})$ and $\text{KCl} \cdot 2\text{PbCl}_2$ and $\text{Pb}_2\text{O}_2\text{Cl}_2$ (Choël et al., 2006; Ettler et al., 2008; Kimbrough & Suffet, 1995; Skeaff et al., 2011; Sobanska et al., 1999).

In-situ sampling in the plume of the smelter in Sudbury, Ontario showed that Cu, Ni, Fe, Mg and Al occur preferentially in the larger fraction ($>2.5 \mu\text{m}$) whereas As, Cd, Pb and Zn occurred preferentially in the smaller fraction (Chan & Lusic (1985). Mineralogical studies of the larger spherical particulates (containing predominantly Cu, Ni, Fe, Mg and Al) showed they are composed of high-temperature silicates, spinel and sulfide phases (Lanteigne et al., 2014; Lanteigne et al., 2012). Wet- and dry-deposition studies using aircraft, ground collectors, and sampling directly below the smelter plume indicated that precipitation events predominantly scavenged particulates containing Zn, Pb and Cd whereas dry deposition led to the preferential depositions of particulates containing Cu, Ni, Fe, Mg and Al (Chan & Lusic, 1985). These observations suggest that larger spherical particulates are less affected by precipitation than smaller particles, which are preferentially washed out of the smelter plume during precipitation (Mantha et al., 2012a; Mantha et al., 2012b). The enhanced wet deposition of smaller metal-bearing arsenates and sulfates closer to the smelter in Sudbury was confirmed by Mantha et al. (Mantha et al., 2012a; Mantha et al., 2012b) who characterized the chemical composition of black rock-coatings around the Ni-smelter in Sudbury, Ontario, Canada. Black rock-coatings form on the surface of bedrock due to the interaction of silicate minerals with sulfuric acid. These coatings are highly resistant to weathering and thus can preserve embedded smelter particulates as well as the S-isotope composition of the acidic rain (Mantha et al., 2012a; Mantha et al., 2012b). The authors argued that the enhanced wet deposition of arsenate-bearing PM resulted in higher As : Ni ratios closer to the smelter in Sudbury and that the subsequent depletion of the smaller As-bearing PM in the smelter plume caused a decrease in this ratio with distance to the smelter (Fig. 10a).

Two mechanisms are involved in the wet deposition of PM: rainout (in-cloud scavenging) and washout (below-cloud scavenging). The two processes are

distinct in terms of the aerosol scavenging mechanism: rainout involves cloud-condensation-nuclei activation of aerosols under super-saturation conditions above the cloud base, whereas washout is the collection of aerosols by falling hydrometeors (Kajino & Aikawa, 2015). For polluted areas, such as the smelter-impacted areas of Sudbury or Flin Flon, the below-cloud wet scavenging can be the main sink of particles during wet deposition (Ge et al., 2021; Sigg et al., 2000). Here, the washout of submicron particles (accumulation or fine-mode particles with diameters of around 100 nm) is slow owing to their gentler Brownian motion and smaller inertia, the so-called Greenfield gap (Greenfield, 1957), whereas the washout of water-soluble gases can be fast, and thus, can scavenge the gases at much faster rate than the submicron aerosols (Jylhä, 1999) (Jylhä, 2001). Hence, the observed enhanced wet deposition of the smaller Zn-, Pb- Cd-As-bearing PM from the Sudbury smelter plume likely comprised soluble particles in the 500 nm to 2.5 μm size range.

Although a wet deposition study was not conducted for the smelter-plume in Flin Flon, the following considerations and observations indicate that precipitation events also resulted in the enhanced wet deposition of smaller or more soluble arsenate-bearing PM within the shadow of the Flin Flon smelter:

- (a) Arsenic occurred primarily in the more volatile smaller size-fraction in the Flin Flon smelter, whereas Zn and Cu (rather than Ni and Cu in Sudbury) were concentrated in the larger size-fraction (Henderson et al., 1998; McMartin et al., 1999);
- (b) The As concentrations in the surficial soils are higher nearer to the smelter than after its deposition peak (Fig. 2e);
- (c) The peak of As deposition occurs closer to the smelter than those for Zn and Cu (Fig. 2);
- (d) Similar to the observations around the Ni-smelter in Sudbury, As : Zn and As : Cu ratios decrease in the surficial soils along the transect with the distance to the smelter (Fig. 10b and c);
- (e) Previous studies on the abundance of Zn, Cu and As in surficial soils along the SE transect also indicate the occurrence of higher As : Zn and As : Cu ratios in close proximity to the smelter (encircled in Fig. 10d-f) as well as at distances greater than 20 km (Fig. 10e-f) (Intrinsik, 2010; Percival & Outridge, 2013); note that the latter

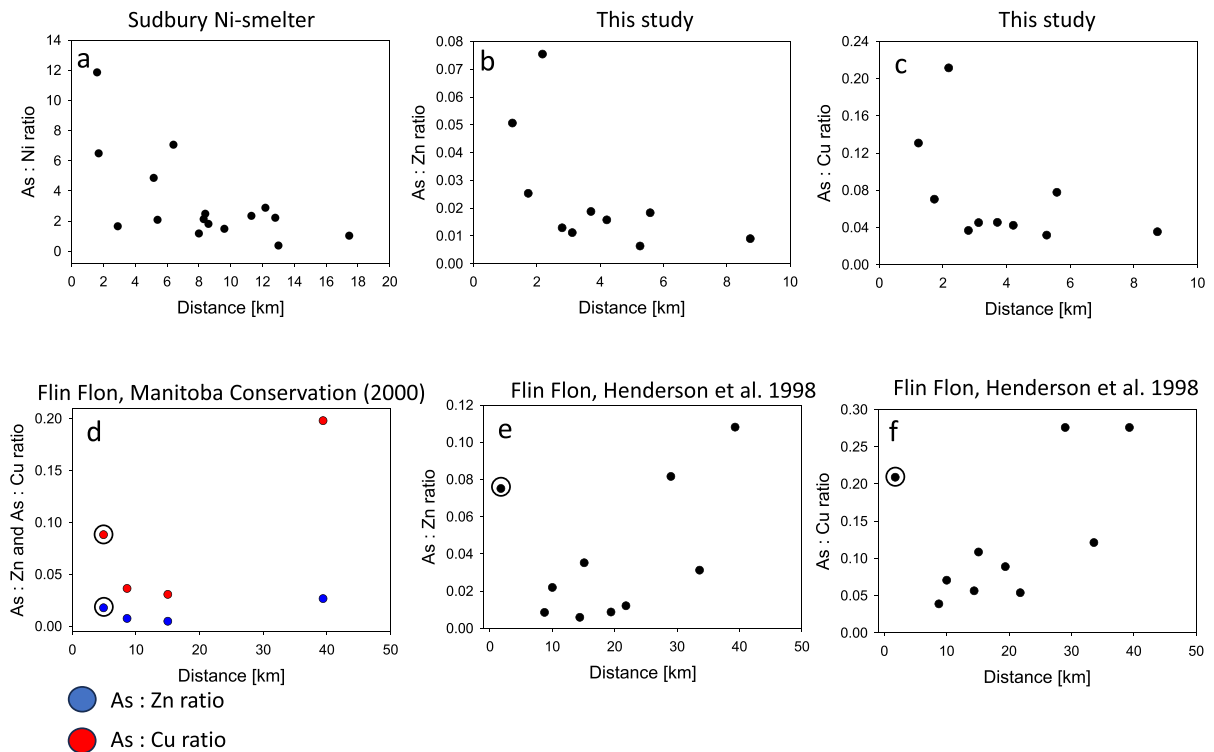


Fig. 10 (a) Ratios of As versus Ni in black rock-coatings in Sudbury Ontario, Canada with distance to the smelters at Copper Cliff and Falconbridge (see Mantha et al. 2012a and b for details); (b)-(f) distance to the smelter versus As : Zn and As : Cu ratios in surficial soils along a SE transect in Flin Flon, Manitoba; (b) As : Zn ratios within 10 km (this study); (c) As : Cu ratios within 10 km (this study); (d) As : Zn and As : Cu

ratios within 40 km from the smelter (Manitoba Conservation study); (e) As : Zn ratios within 50 km from the smelter (Henderson et al. 1998); (f) As : Cu ratios within 50 km from the smelter (Henderson et al. 1998); note that the increase in the As : Zn and As : Cu ratios beyond 20 km is due to the greater long-range transport of the more volatile As

observation also supports the argument by (Henderson et al., 1998 and McMartin et al., 1999) that the volatile element As is transported farther away than Cu and Zn.

Considering that smaller metal-sulfate and metal-arsenate particles

- have a higher solubility than larger spinel-bearing spherical particulates (and thus weather faster in the surficial soils)
- were already deposited as solute species during wet deposition (i.e. were already dissolved in precipitations)
- depict a lower attachment efficiency to mineral surfaces in the soil column than larger particles (Liu et al., 2018),

the greater depth gradients and thus apparent higher mobilities of Cu, Pb and Zn in the soil column of pedon 1 are most likely the result of the wet deposition of a higher proportion of smaller Cu-, Pb- and Zn-sulfate and -arsenate bearing particles or rain drops (relative to the larger spinel-bearing particulates) on the surficial soils of pedon1 than 2.

V. Mineralogical and chemical composition of the soils

Except for the spinel to quartz ratio, there are no major differences in the mineralogical compositions of the surficial horizons of pedon 1 and 2 (detectable with XRD, supplementary data S3). However, there are major differences in the chemical composition as the surficial horizons in pedon 2 are depleted in (Ca+Mg), Fe, and Al with respect to those of pedon 1. These depletions were likely caused by the higher

acidity in pedon 2, which resulted in the dissolution of clay-size Ca-Mg-Fe-Al-silicates and Fe-(hydr)oxides. The enhanced dissolution of the latter minerals cannot explain the lower mobility of Cu, Pb and Zn in pedon 2 but provides an explanation for the higher mobility of As in pedon 2: Arsenic occurs predominantly as the oxy-anions (AsO_4^{3-} or AsO_3^{3-} in acidic oxidized surficial soils. These oxy-anions have a high affinity towards Fe-(hydr)oxides (Fritzsche et al., 2011; Fuller et al., 1993) as those are positively charged under acidic pH conditions. Hence, the two-times higher Fe-concentrations in the surficial horizons of pedon 1 than 2 provide a reasonable explanation for the lower mobility of As in the former than latter pedon.

4.5 Depth Gradients and Leaching Factors for Individual Elements

Closer inspection of Tables 2 and 3 also indicate the following trends:

- (I) In comparison to Cu and Zn, Pb has lower depth gradients in both pedons, lower leaching factors, and occurs in higher proportions in the colloidal fractions of both leachates.
- (II) In comparison to Cu, Zn has a higher depth gradient and leaching factor in pedon 2 and the corresponding surficial soil layers, respectively.

Observation I can be explained by the high solid–water partition coefficient of Pb. Lead has one of the largest first hydrolysis constants of any divalent cation and in the presence of abundant surface sites is quickly removed from solution by adsorption (Hassellöv and von der Kammer, 2008). This high affinity of Pb towards soil colloids (Denaix et al., 2001; Egli et al., 1999) can result in up to 75% of Pb being associated with colloids (Citeau et al., 2003).

The higher depth gradient and leaching factor of Zn relative to Cu (observation II) are only evident in pedon 2 and corresponding surficial soil layers. As these soils occur in proximity to the deposition peak for Zn and Cu, the higher mobility of Zn may be explained by the higher dissolution rate of franklinite relative to cupro-spinel under acidic conditions (Lu and Muir, 1988) and the lower affinity of Zn than Cu towards mineral surfaces and organic matter (Alloway, 2013; Sparks, 2003); the latter is also apparent

in the lower proportion of Zn than Cu in the colloidal fractions of both leachates.

5 Conclusions

This study showed for the first time that the mobilities of Cu, Pb and Zn in a pedon of a remediated (limed) site can be higher than those in a pedon of a non-remediated (acidic) site in the same smelter-impacted area. It indicates specifically that the observed differences in the mobilities of Cu, Pb and Zn at these two sites are predominantly controlled by the solid and chemical nature of deposited particulate matter emitted by the Flin Flon smelter. The knowledge of the type of particulate matter deposited on a soil column during wet or dry conditions came from previous studies using aircraft, ground collectors, and collection of snow samples. These sampling methods in combination with mineralogical studies of unaltered PM at the top of the soil column and the distribution of elements with distance to the smelter must be obtained prior to the interpretation of element distributions within pedons. Similar to the soil studies in the Sudbury area, which showed that an apparent higher mobility of Cu than Ni in pedons was a result of the higher dissolution rate of Cu- versus Ni-spinels under acidic conditions (Lu & Muir, 1988), this study showed that the higher mobility of Cu, Pb and Zn in a pedon at a remediated versus non-remediated site was a product of the enhanced wet deposition of smaller more soluble particles within the shadow of the Flin Flon smelter stack. However, higher mobility of As in the pedon of the non-remediated site (depleted in Fe and Ca + Mg) indicates that mineralogical changes due to the acidification of the soils by smelter emissions can also affect the mobility of elements in pedons.

Acknowledgment We thank Editor in Chief Bin Gao for handling the paper and two anonymous reviewers for their constructive comments. The authors also would like to thank Mozghan Akbari Alavijeh, Sarib Jadoon and Ravi Sidhu for technical assistance and Graeme A. Spiers for his comments on an earlier version of the paper.

Author Contribution M. Schindler wrote the paper; M. Schreckenbach collected the samples; T. Warkentine did the majority of the SEM analyses; Sisara Samaradiwakara did the column experiments and Xinyang Lee did also some of the SEM analyses.

Funding This work was supported by a NSERC discovery grant (RGPIN-2023-04726) to M. Schindler and an undergraduate student research assistant scholarship to M. Schreckenbach.

Data Availability The authors declare that the data supporting the findings of this study are available within the paper and its Supplementary Information files.

Declarations

Competing Interest The authors have no competing interests to declare that are relevant to the content of this article.

References

- Alloway, B. (2013). *Heavy metals in soils: Trace metals and metalloids in soils and their bioavailability* (3rd ed., p. 632). Springer.
- Barrow, N. J., & Whelan, B. R. (1998). Comparing the effects of pH on the sorption of metals by soil and by goethite, and on uptake by plants. *European Journal of Soil Science*, *49*, 683–692. <https://doi.org/10.1046/j.1365-2389.1998.4940683.x>
- Bataillard, P., Cambier, P., & Picot, C. (2003). Short-term transformations of lead and cadmium compounds in soil after contamination. *European Journal of Soil Science*, *54*, 365–376. <https://doi.org/10.1046/j.1365-2389.2003.00527.x>
- Briffa, J., Sinagra, E., & Blundell, R. (2020). Heavy metal pollution in the environment and their toxicological effects on humans. *Heliyon*, *6*, e04691. <https://doi.org/10.1016/j.heliyon.2020.e04691>
- Burt, R., Wilson, M. A., Keck, T. J., Dougherty, B. D., Strom, D. E., & Lindahl, J. A. (2003). Trace element speciation in selected smelter-contaminated soils in Anaconda and Deer Lodge Valley Montana, USA. *Advances in Environmental Research*, *8*, 51–67. [https://doi.org/10.1016/S1093-0191\(02\)00140-5](https://doi.org/10.1016/S1093-0191(02)00140-5)
- Burt, R., Weber, T., Park, S., Yochum, S., & Ferguson, R. (2011). Trace Element Concentration and Speciation in Selected Mining-Contaminated Soils and Water in Willow Creek Floodplain, Colorado. *Applied and Environmental Soil Science*, *2011*, 237071. <https://doi.org/10.1155/2011/237071>
- Caplette, J. N., Schindler, M., & Kyser, T. K. (2015). The black rock coatings in Rouyn-Noranda, Québec: fingerprints of historical smelter emissions and the local ore. *Canadian Journal of Earth Sciences*, *52*, 952–965. <https://doi.org/10.1139/cjes-2015-0064>
- Carrillo-González, R., Šimůnek, J., Sauvé, S. & Adriano, D. (2006). *Mechanisms and Pathways of Trace Element Mobility in Soils*. Advances in Agronomy, Academic Press, pp. 111–178
- Chan, W. H., & Lusia, M. A. (1985). Post-superstack sudbury smelter emissions and their fate in the atmosphere: An overview of the sudbury environment study results. *Water, Air, and Soil Pollution*, *26*, 43–58. <https://doi.org/10.1007/BF00299487>
- Choël, M., Deboudt, K., Flament, P., Lecornet, G., Perdrix, E., & Sobanska, S. (2006). Fast evolution of tropospheric Pb- and Zn-rich particles in the vicinity of a lead smelter. *Atmospheric Environment*, *40*, 4439–4449. <https://doi.org/10.1016/j.atmosenv.2006.04.027>
- Chopin, E. I. B., & Alloway, B. J. (2007). Trace element partitioning and soil particle characterisation around mining and smelting areas at Tharsis Riotinto and Huelva, SW Spain. *Science of The Total Environment*, *373*, 488–500. <https://doi.org/10.1016/j.scitotenv.2006.11.037>
- Cîteau, L., Lamy, I., van Oort, F., & Elsass, F. (2003). Colloidal facilitated transfer of metals in soils under different land use. *Colloids and Surfaces A: Physicochemical and Engineering Aspects*, *217*, 11–19. [https://doi.org/10.1016/S0927-7757\(02\)00554-X](https://doi.org/10.1016/S0927-7757(02)00554-X)
- de Caritat, P., Reimann, C., Chekushin, V., Bogatyrev, I., Niskavaara, H., & Braun, J. (1997). Mass Balance between Emission and Deposition of Airborne Contaminants. *Environmental Science & Technology*, *31*, 2966–2972. <https://doi.org/10.1021/es970193z>
- Denaix, L., Semlali, R. M., & Douay, F. (2001). Dissolved and colloidal transport of Cd, Pb, and Zn in a silt loam soil affected by atmospheric industrial deposition. *Environmental Pollution*, *114*, 29–38. [https://doi.org/10.1016/S0269-7491\(00\)00204-9](https://doi.org/10.1016/S0269-7491(00)00204-9)
- Eckley, C. S., Blanchard, P., McLennan, D., Mintz, R., & Sekela, M. (2015). Soil–Air Mercury Flux near a Large Industrial Emission Source before and after Closure (Flin Flon, Manitoba, Canada). *Environmental Science & Technology*, *49*, 9750–9757. <https://doi.org/10.1021/acs.est.5b01995>
- Egli, M., Fitze, P., & Oswald, M. (1999). Changes in heavy metal contents in an acidic forest soil affected by depletion of soil organic matter within the time span 1969–93. *Environmental Pollution*, *105*, 367–379. [https://doi.org/10.1016/S0269-7491\(99\)00040-8](https://doi.org/10.1016/S0269-7491(99)00040-8)
- Ettler, V., Šebek, O., Grygar, T., Klementová, M., Bezdička, P., & Slavíková, H. (2008). Controls on Metal Leaching from Secondary Pb Smelter Air-Pollution-Control Residues. *Environmental Science & Technology*, *42*, 7878–7884. <https://doi.org/10.1021/es801246c>
- Franzin, W. G., McFarlane, G. A., & Lutz, A. (1979). Atmospheric fallout in the vicinity of a base metal smelter at Flin Flon Manitoba, Canada. *Environmental Science & Technology*, *13*, 1513–1522.
- Freedman, B., & Hutchinson, T. (2011). Pollutant inputs from the atmosphere and accumulations in soils and vegetation near a nickel-copper smelter at Sudbury Ontario, Canada. *Canadian Journal of Botany*, *58*, 108–132. <https://doi.org/10.1139/b80-014>
- Fritzsche, A., Rennert, T., & Totsche, K. U. (2011). Arsenic strongly associates with ferrihydrite colloids formed in a soil effluent. *Environmental Pollution*, *159*, 1398–1405. <https://doi.org/10.1016/j.envpol.2011.01.001>
- Fuller, C. C., Davis, J. A., & Waychunas, G. A. (1993). Surface chemistry of ferrihydrite: Part 2 Kinetics of arsenate adsorption and coprecipitation. *Geochimica et Cosmochimica Acta*, *57*, 2271–2282. [https://doi.org/10.1016/0016-7037\(93\)90568-H](https://doi.org/10.1016/0016-7037(93)90568-H)

- Ge, B., Xu, D., Wild, O., Yao, X., Wang, J., Chen, X., Qixin, T., Pan, X., & Wang, Z. (2021). Inter-annual variations of wet deposition in Beijing from 2014–2017: Implications of below-cloud scavenging of inorganic aerosols. *Atmospheric Chemistry and Physics*, 21, 9441–9454. <https://doi.org/10.5194/acp-21-9441-2021>
- Greenfield, S. M. (1957). Rain Scavenging Of Radioactive Particulate Matter From The Atmosphere. *Journal of Meteorology*, 14, 115–125.
- Gregurek, D., Reimann, C., & Stumpfl, E. F. (1998). Mineralogical fingerprints of industrial emissions — an example from Ni mining and smelting on the Kola Peninsula NW Russia. *Science of The Total Environment*, 221, 189–200. [https://doi.org/10.1016/S0048-9697\(98\)00293-9](https://doi.org/10.1016/S0048-9697(98)00293-9)
- Gregurek, D., Melcher, F., Pavlov, V. A., Reimann, C., & Stumpfl, E. F. (1999). Mineralogy and mineral chemistry of snow filter residues in the vicinity of the nickel-copper processing industry Kola Peninsula, NW Russia. *Mineralogy and Petrology*, 65, 87–111. <https://doi.org/10.1007/BF01161578>
- Hamilton, J. G., Farrell, R. E., Chen, N., Feng, R., Reid, J., & Peak, D. (2016). Characterizing Zinc Speciation in Soils from a Smelter-Affected Boreal Forest Ecosystem. *Journal of Environmental Quality*, 45, 684–692. <https://doi.org/10.2134/jeq2015.03.0145>
- Harter, R., Naidu, R. (2001) An Assessment of Environmental and Solution Parameter Impact on Trace-Metal Sorption by Soils. *Soil Science Society of America Journal - SSSAJ* 65, <https://doi.org/10.2136/sssaj2001.653597x>
- Hassellöv, M., & von der Kammer, F. (2008). Iron Oxides as Geochemical Nanovectors for Metal Transport in Soil-River Systems. *Elements*, 4, 401–406. <https://doi.org/10.2113/gselements.4.6.401>
- Henderson, P. J., & McMartin, I. (1995). Mercury distribution in humus and surficial sediments, Flin Flon, Manitoba, Canada. *Water, Air, and Soil Pollution*, 80, 1043–1046. <https://doi.org/10.1007/BF01189763>
- Henderson, P. J., McMartin, I., Hall, G. E., Percival, J. B., & Walker, D. A. (1998). The chemical and physical characteristics of heavy metals in humus and till in the vicinity of the base metal smelter at Flin Flon Manitoba, Canada. *Environmental Geology*, 34, 39–58. <https://doi.org/10.1007/s002540050255>
- Intrinsik. (2010). *The Flin Flon soils study: an assessment of exposure and human health risks in the Flin Flon area : summary document and integration of results*. Mississauga, Ont., Intrinsik
- Jadoon, S., & Schindler, M. (2022). The role of organic colloids in the sequestration and mobilization of copper in smelter-impacted soils. *Environmental Science: Processes & Impacts*, 24, 945–959. <https://doi.org/10.1039/D1EM00539A>
- Jadoon, S., Schindler, M., Wirth, M. G., Qafoku, O., Kovarik, L., & Perea, D. E. (2022). Atom probe tomography and transmission electron microscopy: a powerful combination to characterize the speciation and distribution of Cu in organic matter. *Environmental Science: Processes & Impacts*, 24, 1228–1242. <https://doi.org/10.1039/D2EM00118G>
- Jylhä, K. (1999). Relationship between the Scavenging Coefficient for Pollutants in Precipitation and the Radar Reflectivity Factor Part I: Derivation. *Journal of Applied Meteorology - J APPL METEOROL*, 38, 1421–1434. [https://doi.org/10.1175/1520-0450\(1999\)038%3c1421:RBTSCEF%3e2.0.CO;2](https://doi.org/10.1175/1520-0450(1999)038%3c1421:RBTSCEF%3e2.0.CO;2)
- Jylhä, K. (2001). Relationship between the scavenging coefficient for pollutants in precipitation and the radar reflectivity factor. (vol 38, pg 1421, 1999). *Journal of Applied Meteorology*, 40, 850–851. [https://doi.org/10.1175/1520-0450\(2001\)040%3c0850:C%3e2.0.CO;2](https://doi.org/10.1175/1520-0450(2001)040%3c0850:C%3e2.0.CO;2)
- Kajino, M., & Aikawa, M. (2015). A model validation study of the washout/rainout contribution of sulfate and nitrate in wet deposition compared with precipitation chemistry data in Japan. *Atmospheric Environment*, 117, 124–134. <https://doi.org/10.1016/j.atmosenv.2015.06.042>
- Kimbrough, D. E., & Suffet, I. (1995). Off-Site Forensic Determination of Airborne Elemental Emissions by Multi-Media Analysis: A Case Study at Two Secondary Lead Smelters. *Environmental Science & Technology*, 29, 2217–2221. <https://doi.org/10.1021/es00009a010>
- Knight, R. D. & Henderson, P. J. (2003). Characterization of smelter dust from the mineral fraction of humus and a comparison with other medium collected around Rouyn-Noranda, Quebec, Canada. In *International Symposium on Environmental Geochemistry (6th :2003 :Edinburgh, Scotland) Geochemistry (ISEG)* (pp. 42–42).
- Knight, R. D., & Henderson, P. J. (2006). Smelter dust in humus around Rouyn-Noranda, Québec. *Geochemistry: Exploration, Environment, Analysis*, 6, 203–214. <https://doi.org/10.1144/1467-7873/05-087>
- Koptsik, G. (2014). Modern approaches to remediation of heavy metal polluted soils: A review. *Eurasian Soil Science*, 47, 707–722. <https://doi.org/10.1134/S1064229314070072>
- Kretzschmar, R., Borkovec, M., Grolimund, D., & Elimelech, M. (1999). Mobile Subsurface Colloids and Their Role in Contaminant Transport. In D. L. Sparks (Ed.), *Advances in Agronomy, Academic Press* (pp. 121–193). ISSN.
- Lanteigne, S., Schindler, M., McDonald, A. M., Skeries, K., Abdu, Y., Mantha, N. M., Murayama, M., Hawthorne, F. C., & Hochella, M. F. (2012). Mineralogy and Weathering of Smelter-Derived Spherical Particles in Soils: Implications for the Mobility of Ni and Cu in the Surficial Environment. *Water, Air, & Soil Pollution*, 223, 3619–3641. <https://doi.org/10.1007/s11270-012-1135-3>
- Lanteigne, S., Schindler, M., & McDonald, A. (2014). Distribution of metals and metalloids in smelter-derived particulate matter in soils and mineralogical insights into their retention and release in a low-T environment. *The Canadian Mineralogist*, 52, 453–471. <https://doi.org/10.3749/canmin.52.3.453>
- Lavkulich, L. M., & Arocena, J. M. (2011). Luvisolic soils of Canada: Genesis, distribution, and classification. *Canadian Journal of Soil Science*, 91, 781–806. <https://doi.org/10.4141/cjss2011-014>
- Liu, F., Xu, B., He, Y., Brookes, P. C., Tang, C., & Xu, J. (2018). Differences in transport behavior of natural soil colloids of contrasting sizes from nanometer to micron and the environmental implications. *Science of The Total Environment*, 634, 802–810. <https://doi.org/10.1016/j.scitotenv.2018.03.381>

- Loon, J. C. V., & Beamish, R. J. (1977). Heavy-Metal Contamination by Atmospheric Fallout of Several Flin Flon Area Lakes and the Relation to Fish Populations. *Journal of the Fisheries Research Board of Canada*, 34, 899–906. <https://doi.org/10.1139/f77-141>
- Lu, Z.-Y., & Muir, D. M. (1988). Dissolution of metal ferrites and iron oxides by HCl under oxidising and reducing conditions. *Hydrometallurgy*, 21, 9–21. [https://doi.org/10.1016/0304-386X\(88\)90013-8](https://doi.org/10.1016/0304-386X(88)90013-8)
- Mantha, N. M., Schindler, M., & Kyser, T. K. (2012a). Silica- and sulfate-bearing rock coatings in smelter areas: Part II. Forensic tools for atmospheric metal(loid)- and sulfur-isotope compositions. *Geochimica et Cosmochimica Acta*, 90, 221–241. <https://doi.org/10.1016/j.gca.2012.05.013>
- Mantha, N. M., Schindler, M., Murayama, M., & Hochella, M. F. (2012b). Silica- and sulfate-bearing rock coatings in smelter areas: Products of chemical weathering and atmospheric pollution I Formation and mineralogical composition. *Geochimica et Cosmochimica Acta*, 85, 254–274. <https://doi.org/10.1016/j.gca.2012.01.033>
- Mantha, H., Schindler, M., & Hochella, M. F. (2019). Occurrence and formation of incidental metallic Cu and CuS nanoparticles in organic-rich contaminated surface soils in Timmins Ontario. *Environmental Science: Nano*, 6, 163–179. <https://doi.org/10.1039/C8EN00994E>
- McCarthy, J. F., & Zachara, J. M. (1989). Subsurface transport of contaminants. *Environmental Science & Technology*, 23, 496–502.
- McFarlane, G. A., & Franzin, W. G. (1978). Elevated Heavy Metals: A Stress on a Population of White Suckers, *Catostomus commersoni*, in Hamell Lake, Saskatchewan. *Journal of the Fisheries Research Board of Canada*, 35, 963–970. <https://doi.org/10.1139/f78-157>
- McFarlane, G. A., & Franzin, W. G. (1980). An Examination of Cd, Cu, and Hg Concentrations in Livers of Northern Pike, *Esox lucius*, and White Sucker, *Catostomus commersoni*, from Five Lakes near a Base Metal Smelter at Flin Flon, Manitoba. *Canadian Journal of Fisheries and Aquatic Sciences*, 37, 1573–1578. <https://doi.org/10.1139/f80-203>
- McMartin, I., Henderson, P. J., & Nielsen, E. (1999). Impact of a base metal smelter on the geochemistry of soils of the Flin Flon region Manitoba and Saskatchewan. *Canadian Journal of Earth Sciences*, 36, 141–160. <https://doi.org/10.1139/e98-001>
- Meadows, M., & Watmough, S. A. (2012). An Assessment of Long-term Risks of Metals in Sudbury: A Critical Loads Approach. *Water, Air, & Soil Pollution*, 223, 4343–4354. <https://doi.org/10.1007/s11270-012-1199-0>
- Mochoruk, J. (2004). *Formidable Heritage: Manitoba's North and the Cost of Development*. University of Manitoba Press.
- Nkongolo, K. K., Spiers, G., Beckett, P., Narendrula, R., Theriault, G., Tran, A., & Kalubi, K. N. (2013). Long-Term Effects of Liming on Soil Chemistry in Stable and Eroded Upland Areas in a Mining Region. *Water, Air, & Soil Pollution*, 224, 1618. <https://doi.org/10.1007/s11270-013-1618-x>
- Outridge, P. M., Rausch, N., Percival, J. B., Shotyk, W., & McNeely, R. (2011). Comparison of mercury and zinc profiles in peat and lake sediment archives with historical changes in emissions from the Flin Flon metal smelter Manitoba, Canada. *Science of The Total Environment*, 409, 548–563. <https://doi.org/10.1016/j.scitotenv.2010.10.041>
- Percival, J. B., & Outridge, P. M. (2013). A test of the stability of Cd, Cu, Hg, Pb and Zn profiles over two decades in lake sediments near the Flin Flon Smelter, Manitoba, Canada. *Science of The Total Environment*, 454–455, 307–318. <https://doi.org/10.1016/j.scitotenv.2013.03.011>
- Rieke-Zapp, D., Poesen, J., & Nearing, M. A. (2007). Effects of rock fragments incorporated in the soil matrix on concentrated flow hydraulics and erosion. *Earth Surface Processes and Landforms*, 32, 1063–1076. <https://doi.org/10.1002/esp.1469>
- Ritchie, G. S. P. (1994). Role of dissolution and precipitation of minerals in controlling soluble aluminum in acidic soils. *Advances in agronomy.*, 53, 47–83.
- Samac, D. A., & Tesfaye, M. (2003). Plant improvement for tolerance to aluminum in acid soils – a review. *Plant Cell, Tissue and Organ Culture*, 75, 189–207. <https://doi.org/10.1023/A:1025843829545>
- Sanborn, P., Lamontagne, L., & Hendershot, W. (2011). Podzolic soils of Canada: Genesis, distribution, and classification. *Canadian Journal of Soil Science*, 91, 843–880. <https://doi.org/10.4141/cjss10024>
- Schindler, M., Lanteigne, S., McDonald, A. M., & Hochella, M. F., Jr. (2016). Evidence of Cu- and Ni-bearing Surface Precipitates and Adsorption Complexes in Remediated Soils At the Nanoscale: a Tem Micro-Raman, and Laser-ablation Icp-ms Study of Mineral Surface Coatings. *The Canadian Mineralogist*, 54, 285–309. <https://doi.org/10.3749/canmin.1500082>
- Schindler, M., Santosh, M., Dotto, G., Silva, L. F. O., & Hochella, M. F. (2022). A review on Pb-bearing nanoparticles, particulate matter and colloids released from mining and smelting activities. *Gondwana Research*, 110, 330–346. <https://doi.org/10.1016/j.gr.2021.07.011>
- Sigg, L., Xue, H., Kistler, D., & Sshönenberger, R. (2000). Size Fractionation (Dissolved, Colloidal and Particulate) of Trace Metals in the Thur River Switzerland. *Aquatic Geochemistry*, 6, 413–434. <https://doi.org/10.1023/A:1009692919804>
- Skeaff, J. M., Thibault, Y., & Hardy, D. J. (2011). A new method for the characterisation and quantitative speciation of base metal smelter stack particulates. *Environmental Monitoring and Assessment*, 177, 165–192. <https://doi.org/10.1007/s10661-010-1627-9>
- Sobanska, S., Ricq, N., Laboudigue, A., Guillermo, R., Brémond, C., Laureys, J., Merlin, J. C., & Wignacourt, J. P. (1999). Microchemical investigations of dust emitted by a lead smelter. *Environmental Science & Technology*, 33, 1334–1339.
- Sparks, D. L. (2003). *Environmental Soil Chemistry*. Elsevier Science.
- Sterckeman, T., Douay, F., Proix, N., & Fourier, H. (2000). Vertical distribution of Cd, Pb and Zn in soils near smelters in the North of France. *Environmental Pollution*, 107, 377–389. [https://doi.org/10.1016/S0269-7491\(99\)00165-7](https://doi.org/10.1016/S0269-7491(99)00165-7)
- Terzano, R., Spagnuolo, M., Vekemans, B., De Nolf, W., Janssens, K., Falkenberg, G., Fiore, S., & Ruggiero, P. (2007). Assessing the Origin and Fate of Cr, Ni, Cu, Zn, Pb, and

- V in Industrial Polluted Soil by Combined Microspectroscopic Techniques and Bulk Extraction Methods. *Environmental Science & Technology*, 41, 6762–6769. <https://doi.org/10.1021/es070260h>
- Wiklund, J. A., Kirk, J. L., Muir, D. C. G., Evans, M., Yang, F., Keating, J., & Parsons, M. T. (2017). Anthropogenic mercury deposition in Flin Flon Manitoba and the Experimental Lakes Area Ontario (Canada): A multi-lake sediment core reconstruction. *Science of The Total Environment*, 586, 685–695. <https://doi.org/10.1016/j.scitotenv.2017.02.046>
- Williamson, B., Har, N., Purvis, O. & Rusu, A. (2012). Preliminary studies of airborne particulate emissions from the Ampellum S.A. copper smelter, Zlatna, Romania. *Studia Universitatis Babeş-Bolyai, Geologia* 48, <https://doi.org/10.5038/1937-8602.48.1.6>
- Zoltai, S. C. (1988). Distribution of base metals in peat near a smelter at Flin Flon Manitoba. *Water, Air, and Soil Pollution*, 37, 217–228. <https://doi.org/10.1007/BF00226493>
- Winterhalder, K. (1995). Dynamics of plant communities and soils in revegetated ecosystems: a Sudbury case study. In J. Gunn (Ed.), *Restoration and recovery of an industrial region: Progress in restoring the smelter-damaged landscape near Sudbury, Canada* (pp. 1586-1598). Springer Verlag.
- Winterhalder, K. (1996). Environmental degradation and rehabilitation of the landscape around Sudbury a major mining and smelting area. *Environmental Reviews*, 4(3), 185–224. <https://doi.org/10.1139/a96-011>
- Wren, C. (2012). Risk assessment and environmental management: A case study in Sudbury, Ontario, Canada. *Progress in Environmental Science, Technology and Management*, 1, 1–450.
- Publisher's Note** Springer Nature remains neutral with regard to jurisdictional claims in published maps and institutional affiliations.
- Springer Nature or its licensor (e.g. a society or other partner) holds exclusive rights to this article under a publishing agreement with the author(s) or other rightsholder(s); author self-archiving of the accepted manuscript version of this article is solely governed by the terms of such publishing agreement and applicable law.